Engineering Structures 297 (2023) 116933

Contents lists available at ScienceDirect

Engineering Structures

journal homepage: www.elsevier.com/locate/engstruct

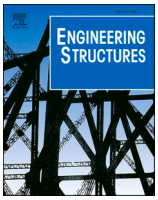

FRP RC beams by collected test data: Comparison with design standard, parameter sensitivity, and reliability analyses

Rabee Shamass [a,*], Ikram Abarkan [b], Felipe Piana Vendramell Ferreira [c]

[a] Division of Civil and Building Services Engineering, School of the Built Environment and Architecture, London South Bank University, UK
[b] Department of Physics, Faculty of Sciences, Abdelmalek Essaadi University, 93002 Tetouan, Morocco
[c] Faculty of Civil Engineering, Federal University of Uberlândia – Campus Santa Mônica, Uberlândia, Minas Gerais, Brazil

ARTICLE INFO

Keywords:
Eurocode 2
Fiber-reinforced polymers
Reinforced concrete
Parameter Influence
Reliability analysis
Sustainability

ABSTRACT

In the last few years, there has been a significant increase in the utilization of Fiber Reinforced Polymer (FRP) materials as reinforcing elements in concrete structures due to their excellent properties. Unlike traditional steel rebars, FRP rebars do not rust, which helps to prevent degradation and deterioration of the concrete structure over time. This growth has resulted in a rise in the application of design regulations for FRP-reinforced concrete (RC) members. There are currently no European standards that offer suggestions about FRP RC structures. This paper aims to assess the load- carrying capacity and deflection of FRP RC beams with large number of test data available against design standards. The results are compared with ACI 440.1 R-06 specifications and EC2 concepts available in fib Bulletin No. 40. It was found that both ACI and EC2 underestimate the shear flexural capacity. Both design codes presented 38% and 62% of the collected data that overestimated and underestimated the calculation of the deflection, respectively. A parameter influence analysis is performed considering the database collected, and a reliability analysis based on Annex D EN 1990 (2002) is conducted. The reliability analysis allowed suggestion new partial safety factors values of 1.45 and 1.65 for moment and shear capacities, respectively, which can be used by design engineering communities.

1. Introduction

Excessive cracks in steel reinforced concrete (RC) infrastructures reduce the overall durability of structures by allowing the penetration of water and aggressive agents, thereby accelerating the deterioration, mainly corrosion, of reinforcing steel. Corrosion reduces the cross-section area of reinforcing steel, resulting in the reduction of the bearing capacity of steel-reinforced concrete. Studies showed that under excessive corrosion, the reinforcing steel suffers a significant loss of ductility [1–2], reduction in yield and ultimate strength, and deterioration in bond properties [3]. Cracking of concrete and the reduction in the cross-sectional area of steel rebar endanger the safety and serviceability of reinforced concrete structures. Unsatisfactory durability of concrete structures not only impacts the economy negatively and causes the repairing expense of deteriorated structures which is almost equal to the cost of construction of new ones, but also industrial, environmental, and social problems also arise because of the reduced reliability and safety. According to estimations released by the UK government's Department for Transport, the annual cost of steel corrosion on highways and trunk road bridges, exclusively in England and Wales, is approximately £616.5 million [4]. Therefore, steel corrosion always remains a continually ongoing research focus.

Steel corrosion is mostly caused by Chloride ions in harsh environments such as in bridges, marine infrastructures and parking facilities along coastlines [5], where steel RC structures are subjected to saltwater or deicing salts. There are a number of protection methods to deal with the corrosion problem in RC members, such as cathodic protection, epoxy-coated steel rebar, or increasing concrete cover thickness [6,7]. However, these methods are not radical solutions to the steel reinforcement corrosion problem, and they are reactive and add to material usage in design. The use of fibre-reinforced polymers (FRP) such aramid FRP (AFRP), carbon FRP (CFRP), and glass FRP (GFRP) is an effective alternative to traditional steel reinforcement, which recently have gained popularity in construction industry.

FRPs are composite materials made of a matrix and reinforcement fibres; according to various specifications (e.g., ISIS CANADA Design Manual No.3 2007 [8]), the fibre-volume percentage must typically be higher than 55% to fulfil the reinforcement role [7]. Externally bonded

* Corresponding author.
E-mail address: shamassr@lsbu.ac.uk (R. Shamass).

https://doi.org/10.1016/j.engstruct.2023.116933
Received 18 April 2023; Received in revised form 31 July 2023; Accepted 19 September 2023
Available online 3 October 2023

fibre-reinforced polymers (FRPs) have been used for retrofitting reinforced concrete (RC) beams in shear [81,82] and flexural [83]. In general, FRPs have been used as reinforcement materials in civil engineering since the 1980 s, due to their low density, good mechanical performance, sustainability and affordability, in addition to their high resistance to corrosion in comparisons to steel. Another type of FRPs that has evolved, in recent years, and has drawn a lot of interest is Basalt FRP (BFRP), owing to its durability, sustainability and cost savings with respect to Glass and Carbon FRPs [9].

Compared to steel, FRPs have a variety of advantages. For instance, they are easier and less costly to produce as no additives are used during the fabrication process, particularly BFRP [10]. Additionally, FRP materials have a high strength-to-weight ratio, which lowers transportation cost. In terms of durability, FRPs are highly resistant to aggressive environments due to their excellent resistance to corrosion and chemical effects. For example, Duo et al. [11] studied the durability of GFRP and BFRP bars in harsh environmental conditions, including saline, alkaline and acid, using existing test data available in the literature. They found that the matrix type, fibre volume fraction, and exposure temperature are the main factors influencing durability. Besides, both materials performed best in the salt solution, followed by the acid solution, water, and alkaline solution. The durability and mechanical performance of GFRP in an aggressive environment at ambient temperature was also investigated by Lu et al. [12]. According to the test results, GFRP has good durability in saline solutions and tap water followed by alkaline solutions, where strength degradation was observed in the latter. For instance, for 11.2 mm GFRP bar diameter, the tensile strength decreases by 20%, 9.1% and 10.7% when exposed to Alkaline, Saline, and Tap water solutions at 90 days, respectively. They also found that resistance to strength deterioration increases as the diameter of the bar increases. For instance, the tensile strength of the 11.2 mm and 15.6 mm decreased by 20% and 8.3%, respectively, when exposed to Alkaline solution for 90 days. Regarding sustainability, the production of FRPs emits less carbon dioxide than traditional steel [13], thereby minimizing environmental effects. Moreover, FRPs outperform steel because they are lighter, which reduces construction costs and accelerate the construction rate. Furthermore, because of their high strength and stiffness (for CFRP), FRP RC structures require less reinforcing material to perform similarly to their steel RC counterpart, thus lowering resource consumption and reducing pollution [14]. In terms of mechanical properties, FRPs have a material behaviour that is distinguished by a low elastic modulus (e.g., the elastic modulus of GFRP typically ranges from 35 to 45 GPa [15]), no yielding point (i.e., linear behaviour up to failure), but higher tensile strength than steel.

Numerous experimental research studies have been conducted to understand the structural behaviour (bending and shear) of concrete elements reinforced with FRP. An illustration would be the research studies given in references [1,5–7,9,15–66], where several parameters were taken into account when conducting the experiment (e.g., concrete strength, flexural and shear reinforcement ratio and type, and shear span-to-depth ratio, etc.). With regards to the flexural behaviour, Shamass and Cashell [1] examined the bending characteristics of simply supported BFRP beams and showed that, for the same reinforcement ratio, BFRP reinforced beams had a higher moment capacity than steel RC beams, however, wider cracks, larger deflections and lower bending stiffness were observed. Abed et al. [9] conducted an experimental study on the flexural behaviour of simply-supported concrete beams reinforced with BFRP, CFRP, or steel. For a comparable reinforcement ratio, FRP RC beams were found to have smaller crack widths, higher moment capacity, and better deflection behaviour than Steel RC beams. One other study conducted by Balendran et al. [21] on sand-coated GFRP reinforced beams and mild steel RC beams, revealed that GFRP RC beams had higher deflection, and 1.4–2.0 times higher ultimate strength than that for steel RC beams. With regards to the shear behaviour, Tomlinson and Fam [22] examined the shear performance of BFRP RC beams with and without BFRP shear reinforcement and found that all of these beams failed in shear, reaching 90–96% and 55–58% of flexural capacity, respectively. On the other hand, the ultimate capacity was observed to increase as the BFRP flexural reinforcement ratio increased in both test configurations. Furthermore, it was found that the load–deflection behaviour in the service load range was unaffected by the type of shear reinforcement (i.e., steel, BFRP, or no shear reinforcement). Said et al. [7] conducted another study on the shear behaviour of GFRP RC beams with and without GFRP shear reinforcement and revealed that adding GFRP as shear reinforcement increases the ultimate shear capacity by 41% and 82% of the beam without stirrups. It is worth pointing out that the capacity of FRP RC members was influenced by the concrete strength, RC member geometry, type of FRP reinforcement, reinforcement ratio, and shear-to-effective depth ratio.

The design of FRP reinforced concrete members can be assisted by different international standards, including the American ACI 440.1 R-06 [67], the Canadian CSA S806-02 [68], and the Russian SP295 [69]. Nevertheless, there is currently, up to this date, no European standard available to assess, for example, the load capacity or deflection of FRP RC structures. The corresponding technical reference is fib Bulletin No. 40 [70], which applies the Eurocode 2 (EC2) [71] methodology, is frequently used in the design of FRP reinforced structures. However, none of the aforementioned standards and guidelines have yet to make any recommendations for BFRP reinforcement material [1,9]. Hence, several attempts have been made to investigate the accuracy international standards to predict the load-bearing capacity as well as the deflections to obtain safe and sustainable design. For examples, research studies found that ACI-440.1R-06 [67] underestimates the flexural capacity of FRP RC beams [9,15,31], underestimates the shear capacity with and without stirrups [7,29,30,32,38,39], and underestimates deflection at service loading [5,24–26,33]. Similarly, research investigation concluded that CSA S806-02 [68] underestimates the flexural capacity of FRP RC beams [1], underestimates the shear capacity with and without stirrups [34,42,46], and overestimates the deflection at service loading [1,24]. On the other hand, only a limited number of studies have examined the performance of EC2 [71] in predicting the flexural behaviour of FRP RC beams [1,15,36]. For example, Barris et al. [15] used 12 test data to evaluate the applicability of EC2 equations for GFRP RC beams at the serviceability and ultimate limit states. They revealed that EC2 accurately predicts flexural behaviour up to service load while providing conservative results at the ultimate limit state. Shamass and Cashell [1] found that EC2 gives the most accurate predictions for the deflection, while slightly overestimates the flexural capacity of BFRP RC beams. More recently, Borzovic et al [84] assessed the accuracy and reliability of the of the 2nd generation of EC2 for predicting the shear capacity of GFRP RC one-way slabs based on statistical evaluations. They concluded that the design provision that was originally developed for predicting the shear capacity of steel RC members can be successfully applied to GFRP RC members by adjustment of the reinforcement ratio with modulus ratio (GFRP modulus-to-Steel modulus ratio). To authors' knowledge, no research with sufficient data has been conducted to assess EC2 in predicting the shear and flexural behaviour of FRP RC beams.

Even though the structural behaviour of FRP reinforced beams has been the subject of extensive experimental investigations (e.g., [1,5–7,9,15–66]) little work has been done to assess the accuracy of the existing design codes in predicting the load capacity and deflection of FRP-RC beams using large number of experimental data. The international design code equations do not accurately predict flexural/shear behaviour of FRP RC members. Furthermore, there is little research studies have been done to investigate the applicability of the design concepts in the EC2 [71] to predict flexural/shear behaviour of FRP-RC beams. This work aims at evaluating the load carrying capacity and deflection behaviour of simply-supported beams reinforced with high and normal strength concrete in accordance with ACI 440.1 R-06 [67] specifications and EC2 concepts available in fib Bulletin No. 40 [70] using a large number of the available test data in the literature between

1993 and 2022. The key parameters include the beam dimensions (i.e., beam with (b), effective depth(d), and shear span (a), compressive strength of concert (f_c), tensile strength (f_{fu}) and Young modulus of longitudinal reinforcement (E_f) and that of shear reinforcement (E_{fv}), longitudinal and transverse reinforcement ratio , (ρ_f) and (ρ_v) respectively, and type (GFRP, CFRP, BFRP or AFRP) for the main reinforcement and FRP or steel for shear reinforcement. The accuracy of the existing EC2 concepts in fib Bulletin No. 40 [70], has been evaluated using 336 experimental data points to estimate the maximum load capacity, and 195 experimental data points were used to compare with the estimated deflection for FRP reinforced beams at service loading. The obtained predicted results from ACI 440.1 R-06 standard [67] are also provided and used for comparison. Finally, design suggestions according to EC2 [71] for FRP-RC beams are provided in light of the findings obtained in this research paper.

2. Collected test data

To provide relevant experimental data for this study, the published literature on simply supported FRP RC beams was carefully examined. A total of 336 test data from 53 references on ultimate load and 195 experimental data points on load–deflection in 36 references have been collected. Three points, from the load–deflection curve, have been taken into consideration: the curve's origin, the corresponding deflection at 67%, and 90% of the ultimate load P_u. The database includes beams with high and normal concrete strength, with and without transverse (shear) reinforcement. FRP materials are used for the main reinforcement, while, in the case of beams with stirrups, steel or FRPs are used for shear reinforcement. Additional elements are also considered, such as reinforcement ratio, the concrete cover, and the beam size. Table 1 provides characteristics about the FRP RC beams that served as the database, and Fig. 1 shows the statistical analysis, considering the number of observations per variation of physical and geometric parameters relationship of the collected tests via mean, standard deviation, maximum and minimum values of each parameter analysed, in which No. is number of samples, f_c is the compressive strength of concrete, b is beam with, d: is the effective depth, a is the shear span, ρ_f and ρ_v are the reinforcement ratio of longitudinal and shear stirrups, respectively, f_{fu} is the ultimate strength of FRP, E_f and E_{fv} are the Young modulus of longitudinal and shear FRP, respectively, f_u^{FRP} and f_u^s are the ultimate strength of FRP and steel stirrups, respectively. It is worth mentioning that due to inaccessibility of some paper, the data was retrieved from an alternative reference [72], and therefore were only used for load capacity calculation.

3. Methodology

This section covers the design provisions in ACI 440.1 R-06 [67] and EC2 [71] for FRP-RC simply supported beams, with special emphasis on cracking load, ultimate capacity and deflection response. Depending on the amount of FRP reinforcement and concrete, the failure is classified as flexural (crushing of concrete / rebar rupture) or shear. Considering that FRP rupture occurs suddenly, concrete crushing is generally seen as the most acceptable flexural failure. Nevertheless, both flexural failure modes are generally acceptable for FRP RC design structures as long as the strength and serviceability requirements are respected [1]. Excessive cracking and deflections are both indication of FRP rupture, whereas in the case of concrete crushing, the FRP RC element exhibits high deformation, and the cross-section shows pseudo-plastic behaviour prior to failure [73]. The methodology described in the following subsections was used to calculate the cracking moment, shear and moment capacity, and deflection with respect to EC2 and ACI 440.1 R-06. It is worth pointing out that the partial material factors were taken equal to unity for comparisons with tests results.

3.1. 4.1 Eurocode 2 design

3.1.1. Cracking moment

The bending moment at first visible crack (M_{cr}) for each FRP RC beam is determined using the following equation [70–71]:

$$M_{cr} = \frac{f_r I_g}{y_t} \tag{1}$$

where (I_g) denotes the gross moment of inertia, (y_t) is the vertical distance between the extreme tension fibres and the neutral axis, and (f_r) represents the concrete's modulus of rupture and can be obtained based on EC2, using Eq. (2).

$$f_{r,EC2} = 0.3(f_c)^{2/3} \tag{2}$$

where (f_c) is the cylindrical compressive strength of concrete, which is taken as 0.81 f_{cu} in the current work if cubic strength (f_{cu}) is provided.

3.1.2. Ultimate capacity

The ultimate capacity of FRP-RC beams is defined based on bending and shear capacities. As stated already that the flexural failure can take place due to concrete crashing or rebar rupture, depending on the reinforcement ratio. If the FRP reinforcement ratio ($\rho_f = \frac{A_f}{bd}$) is more than the balanced reinforcement ratio (ρ_b) then the flexural failure occurs due to concrete crashing (i.e., the concrete reaches the ultimate strain capacity), otherwise, the flexural failure is rebar rupture (i.e., the rebar reaches its ultimate tensile capacity). The reinforcement ratio (ρ_f) is assumed to be balanced (ρ_b) when both concrete and FRP longitudinal reinforcement are in such a proportion that concrete crushing and FRP reinforcement failures occur simultaneously.

The balanced reinforcement ratio (ρ_b) can be obtained using the following equation, according to EC2 principles [70]:

$$\rho_{b,EC2} = \frac{\lambda\eta f_c \varepsilon_{cu}}{f_{fu}(\varepsilon_{fu} + \varepsilon_{cu})} \tag{3}$$

where (λ) and (η) are parameters related to the equivalent rectangular stress blocks in the concrete and are equal to 0.8 and 1, respectively, for $f_c \leq 50$ MPa. Otherwise, for $50 < f_c \leq 90$ MPa, the following expressions are used:

$$\lambda = 0.8 - \frac{f_c - 50}{400} \tag{4}$$

$$\eta = 1.0 - \frac{f_c - 50}{200} \tag{5}$$

In these expressions, (ε_{cu}) is the ultimate compressive strain (i.e., crushing strain) of concrete and it is taken accordance to EC2 design, (ε_{fu}) is the ultimate strain in the FRP and is defined as the ratio of the ultimate strength (f_{fu}) to the elastic modulus (E_f) of longitudinal FRP rebar.

If $\rho_f \geq \rho_{b,EC2}$ the flexural failure mode is expected to be concrete crushing, and the flexural moment capacity ($M_{ult,EC2}$) is calculated, based on EC2, as follows:

$$M_{ult,EC2} = \eta f_c b d^2 (\lambda\xi)\left(1 - \frac{\lambda\xi}{2}\right) \tag{6}$$

where

$$\xi = \frac{\varepsilon_{cu}}{\varepsilon_f + \varepsilon_{cu}} \tag{7}$$

and

$$\varepsilon_f = \frac{-\varepsilon_{cu} + \sqrt{\varepsilon_{cu}^2 + \frac{4 f_c \lambda\eta \varepsilon_{cu}}{\rho_f E_f}}}{2} \tag{8}$$

Table 1
Summary of the FRP-RC beams characteristics used in the current study.

References	No.	Beam geometry and concrete strength				Tensile reinforcement				Shear reinforcement			
		f_c(MPa)	b (mm)	d (mm)	a (mm)	ρ_f(%)	f_{fu}(MPa)	E_f(GPa)	Longitudinal reinforcement at tension	ρ_v(%)	Shear reinforcement	f_u^{FRP}(FRP)/ f_u^{s}(Steel) (MPa)	E_{fv}(MPa)
Shamass & Cashell [1]	2	33.53–35.96	125	162	650	0.78	1356–1565	54–56	BFRP	0.80	Steel	523	–
Adam et al. [5]	4	19.85–60.26	120	250–258	1100	0.32–2.26	640	44	GFRP	0.56	Steel	500	–
Theriault & Benmokrane [6]	4	52.1–97.4	130	129.2–147.85	500	1.23–2.83	773	38	GFRP	0.54	Steel	460	–
Abed et al. [9]	10	47.5–70.5	180	182–186	750	0.45–1.84	1028.7–2068	42.8–131	BFRP/CFRP	0.87	Steel	460	–
Barris et al. [15]	2	56.3–61.7	140–160	142–162	600	1.77	995	64.152	GFRP	0.90–1.03	Steel	500	–
Pecce et al. [19]	2	30	500	145	1200	0.7–1.22	600	42	GFRP	0.2	Steel	500	–
Al-Sunna et al. [23]	4	37.67–44.87	150	193.45–221.83	767	0.28–3.93	665–1475	42–133	GFRP/CFRP	0.89	Steel	590	–
Elgabbas et al. [24]	5	42.5	200	233.5–256	1100	0.44–1.72	1162–1189	44.4–48.7	BFRP	0.79	Steel	450	–
Zhang et al. [25]	4	26.3–34	180	187–189	600	0.17–0.70	1075–1204	44.3–49	BFRP	0.56	Steel	335	–
Kassem et al. [26]	11	39.05–40.8	200	232.3–251	875	0.51–2.18	617–1988	36–122	CFRP/GFRP	0.98	Steel	460	–
Pawłowski et al. [28]	2	42.36	200	257.5–258.5	900	0.22–0.62	1185–1485	52.8–56.3	BFRP	0.50	Steel	500	–
Rafi et al. [29]	1	41.71	120	169.25	675	0.69	1676	135.9	CFRP	0.47	Steel	421	–
Alsayed et al. [33]	4	31.3–40.7	200	157.5–247.5	1250	1.15–3.60	700–886	35.63–43.37	GFRP	0.50	Steel	553	–
Sun et al. [35]	2	39.53	220	252–258	600	0.62–1.70	907–2550	46.2–147	BFRP/CFRP	0.57	Steel	500	–
Barris et al. [36]	5	32.1–54.5	140–160	144–164	600	0.98–2.66	1015–1321	63.44–64.63	GFRP	0.90–1.03	Steel	500	–
Oh et al. [37]	7	28.6	180	185–195	680	0.47–0.93	841–1200	42.1–42.80	GFRP	1.45–2.18	Steel	500	–
Kalpana & Subramanian [40]	4	20–60	200	198–202	550	0.99–1.57	600	55	GFRP	0.28	Steel	500	–
Erfan et al. [41]	8	30–60	150	208–213	600	0.31–1.63	1400	56	BFRP	0.45–1.34	Steel	500	–
Yang et al. [44]	1	75.9	230	206	800	1.6	941	48.1	GFRP	0.85	Steel	477	–
Thiagarajan et al. [47]	6	43.88–53.31	152.4	122.29–123.88	508	0.36–0.76	1900	140	CFRP	0.65	Steel	415	–
Khorasani et al. [31]	20	30	250	211–217	800	0.72–1.45	775–825	42–46	GFRP	0.57–1.15	NA/Steel	462–473	–
Tomlinson & Fam [22]	6	48–60	150	250–270	1100	0.13–0.84	1158.5	68.35	BFRP	0.17–0.68	NA/Steel/ FRP	485–1158.5	68.35
Duranovic et al. [48]	9	24—34.72	150	215.25—223.25	512–767	0.88–1.33	1000	45	GFRP	0.38–1.68	NA/Steel/ FRP	600–1000	45
Toutanji & Deng [20]	3	35	180	255–268	1200	0.53–1.10	695	40	GFRP	1.26	FRP	695	40
Jumaa et al. [27]	4	73.4	200	234–408	610–1070	3.0	1089	58	BFRP	0.25–0.63	FRP	1100	56
Wang et. [34]	1	32.5	120	212	700	0.88	826	109.7	CFRP	0.40	FRP	826	109.7
Said et al. [7]	10	19.85–60.26	120	250	500	1.13–2.26	640	44	GFRP	0.39–0.84	NA/FRP	640	44
Massam [43]	6	35–49	450	404–937.5	3050	0.48–2.23	517	40.8	GFRP	0.079–0.16	NA/FRP	517	40.8
Zhao et al. [46]	9	34.3	150	250	750–1000	1.51–3.02	1124	105	CFRP	0.41	NA/FRP	1100–1300	39–100
Issa et al. [52]	9	35.9	200–300	165–270	397.5–1190	0.78–3.97	1050–1070	48–53	BFRP	0.31	NA/FRP	1070	53
Nagasaka et al. [55]	12	22.9–36.7	250	253–265	480.7–503.5	1.9	1000*	56	AFRP	0.5–1.5	NA/FRP	690**	56
Maruyama & Zhao [56]	13	27.5–38.3	150	250	750	0.55–2.11	1170**	94	CFRP	0.12–0.24	NA/FRP	690**	94
Vijay et al. [57]	6	31–44.8	150	265	503.5	0.64–1.43	690**	54	GFRP	0.62–0.93	NA/FRP	690**	54
Maruyama [58]	5	29.5–34	150–300	250–500	625–1250	1.07	1170**	10	CFRP	0.43–1.28	NA/FRP	690**	10
Alkhrdaji et al. [59]	3	24.1	178	279	750.5	2.3	690**	40	GFRP	0.40—0.52	NA/FRP	690**	40
Niewels [60]	8	43–48	300	412–441	1302–1323	3.25—3.65	690**	63	GFRP	0.14–0.54	NA/FRP	690**	63
Razaqpur et al. [30]	7	40.5–49	200	225	410–950	0.22–0.78	2250	145	CFRP	–	NA	NA	–
Ashour [32]	12	27.54–47.79	150	164–267	666.67	0.14–1.38	650–705	32–38	GFRP	–	NA	NA	–

(*continued on next page*)

Table 1 (*continued*)

References	No.	Beam geometry and concrete strength				Tensile reinforcement				Shear reinforcement			
		f_c(MPa)	b (mm)	d (mm)	a (mm)	ρ_f(%)	f_{fu}(MPa)	E_f(GPa)	Longitudinal reinforcement at tension	ρ_v(%)	Shear reinforcement	f_u^{FRP}(FRP)/ f_u^s(Steel) (MPa)	E_{fv}(MPa)
El Refai & Abed [38]	8	49	152	206–220	545–726	0.33–1.45	1168	50	BFRP	–	NA	NA	–
Kim & Jang [39]	12	30–40.3	150–200	213.5–215.5	625–750	0.30–0.83	900–2130	40–147.90	CFRP/ GFRP	–	NA	NA	–
Alam & Hussein [42]	10	37.4–44.7	250	305–460	762.5–1150	0.18–0.92	751–1899	46.3–144	GFRP/CFRP	–	NA	NA	–
Matta et al. [45]	5	29.5–59.7	114–457	147–883	457–2743	0.60	517	40.7–40.8	GFRP	–	NA	NA	–
Tariq et al. [49]	6	34.1—43.2	130–160	310–346	950–1150	0.73–1.56	674–1596	42–120	GFRP/CFRP	–	NA	NA	–
Yost et al. [50]	6	36.3	178—279	224–225	914	1.10–2.22	689.5	40.34	GFRP	–	NA	NA	–
Tureyen et al. [51]	2	34.5	457	360	1224	0.96	592.9–606.7	37.58–40.54	GFRP	–	NA	NA	–
Ali et al. [53]	12	13–33.5	130	195	450–600	0.30–0.91	770	51.5	GFRP	–	NA	NA	–
Zeidan et al. [54]	4	24–54	150	280	350–700	0.11–0.21	2840	148	CFRP	–	NA	NA	–
Tottori & Wakui [61]	9	44.5–46.9	200	325	1040	0.7–0.9	1170**	58–192	CFRP	–	NA	NA	–
Nakamura & Higai [62]	2	22.7	300	150	***	1.3–1.8	690**	29	GFRP	–	NA	NA	–
Mizukawa et al. [63]	7	28.2–34.7	200–305	158–260	***	1.3	1170**/ 690**	13–40	CFRP/GFRP	–	NA	NA	–
Lubell et al. [64]	1	40	450	970	***	0.5	690**	40	GFRP	–	NA	NA	–
El-Sayed et al. [65]	8	40	1000	154–165	***	0.4–2.6	1170**/ 690**	40–114	CFRP/GFRP	–	NA	NA	–
El-Sayed et al. [66]	6	43.6–55	250	326	***	0.9–1.7	1170**/ 690**	40–130	CFRP/GFRP	–	NA	NA	–

* assumed minimum value in fib Bulletin No. 40 [70];
** assumed minimum value recommended in ACI;
*** data inaccessible.

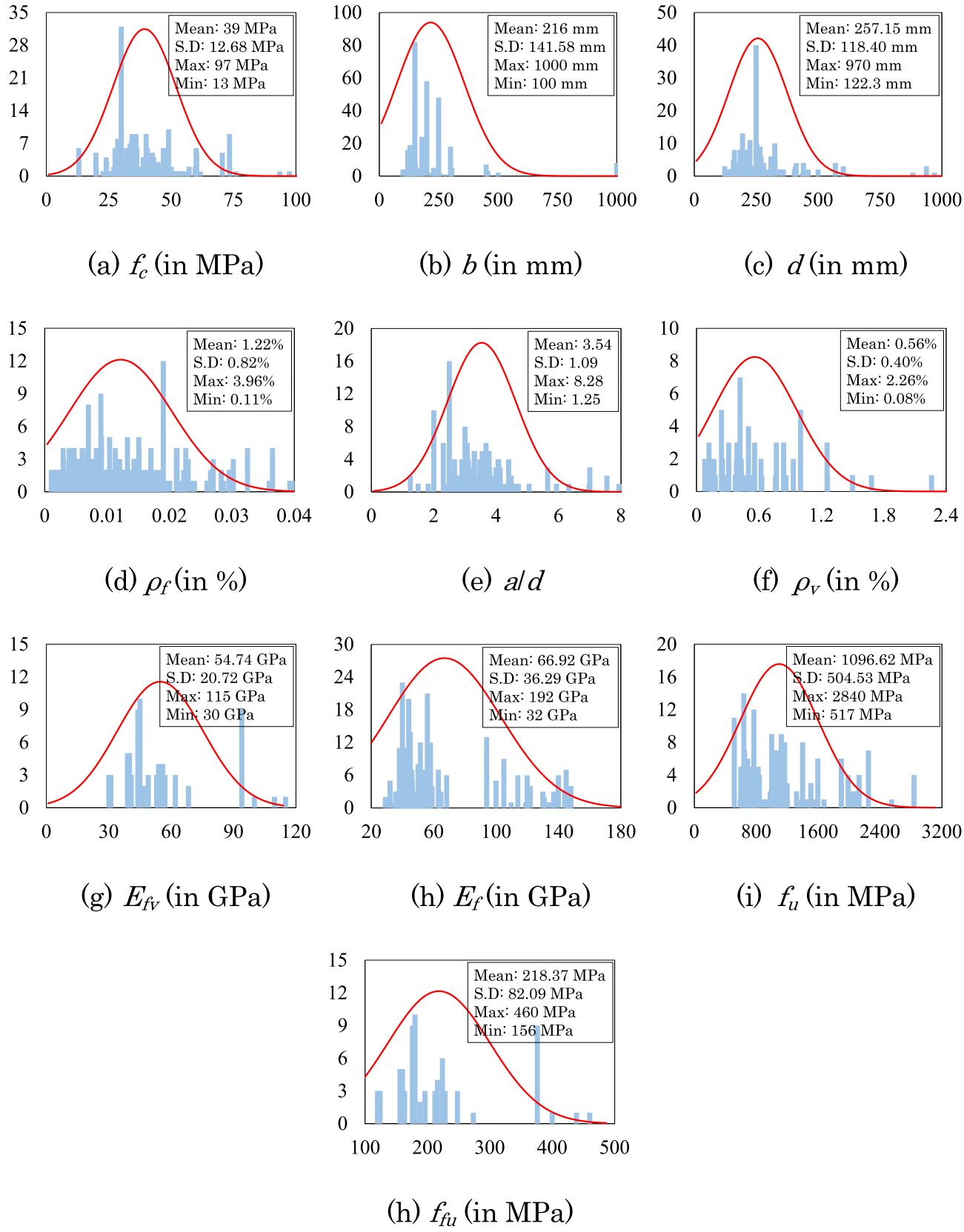

Fig. 1. Statistical analysis of geometric and physical parameters of collected data.

With ε_f is the strain in FRP material when concrete reach the crushing strain.

Alternatively, if $\rho_f \leq \rho_{b,EC2}$ then the FRP rupture is expected, and the strain in the main FRP rebar reaches that ultimate strain, but the strain in the concrete is below the crushing strain. According to the EC2 framework in [70], the corresponding flexural moment capacity $(M_{ult,EC2})$ is defined as:

$$M_{ult,EC2} = A_f f_{fu}\left(1 - \frac{\xi}{2}\right) \tag{9}$$

where (A_f) represent the cross-sectional area of FRP.

To determine the concrete compressive strain (ε_c) at which the FRP fails, it is necessary to use trial and error procedures to solve the equilibrium equation, this is obtained by solving the following equations:

$$\xi = \frac{\varepsilon_c}{\varepsilon_{fu} + \varepsilon_c} \tag{10}$$

$$F_C = F_T \rightarrow bd\xi \frac{\int_0^{\varepsilon_c} \sigma_c d\varepsilon_c}{\varepsilon_c} = A_f f_{fu} \tag{11}$$

where σ_c, the compressive stress in concrete, is calculated using these expressions:

$$\sigma_c = f_c\left[1 - \left(1 - \frac{\varepsilon_c}{\varepsilon_{c2}}\right)^n\right] \text{for } 0 \leq \varepsilon_c \leq \varepsilon_{c2} \tag{12}$$

$$\sigma_c = f_c \text{ for } \varepsilon_{c2} \leq \varepsilon_c \leq \varepsilon_{cu\,2} \tag{13}$$

The values provided by EC2 [71] are used for concrete strains (ε_{cu2}) and (ε_{c2}), the exponent (n) corresponds to the characteristic strength of concrete.

On the other hand, the total shear capacity (V) represents the sum of the shear capacities of the concrete (V_{cf}) and the stirrups (V_f).

$$V = V_{cf,EC2} + V_{f,EC2} \tag{14}$$

The concrete contribution in shear (V_{cf}) can be calculated using the following equation which takes into considerations the effect different axial stiffness of flexural FRP reinforcement [70]:

$$V_{cf,EC2} = 0.12bd\left(1 + \sqrt{\frac{200}{d}}\right)\left(100\frac{A_f}{bd}\frac{E_f}{E_s}\phi_\varepsilon f_c\right)^{1/3} \tag{15}$$

With $\left(1 + \sqrt{\frac{200}{d}}\right) \leq 2$

where (ϕ_ε) is the ratio of the maximum allowable strain in the FRP reinforcement (ε_f), which is equal to 0.0045, and the elastic strain of the steel $(\varepsilon_y = 0.2\%)$.

The stirrups contribution (V_f) can be calculated using the same method as for steel RC but with the assumption that the strut angle is 45°, as observed experimentally in many research studies [7,20,27,43,46] and considering the level of stresses in the shear link is controlled by maximum strain developed in the shear reinforcement. The initial recommendation of the limiting strain was based on the yield stress of steel (between 0.2% and 0.25%). However, it was recommended by members of FIB TG 9.3 [70] and based on experimental evidence that higher limiting strains can be utilized up to 0.45%. Hence, the stress developed in the shear link is:

$$f_{fv} = 0.0045E_{fv} \tag{16}$$

The shear contribution of shear reinforcement links is then calculated as:

$$V_{f,EC2} = \frac{A_{fv} f_{fv} d}{s} \tag{17}$$

with E_{fv}, A_{fv}, s refer to the Young's modulus, cross-sectional area and spacing of FRP stirrups.

3.1.3. Deflections

The expression given in Eq. (18) is provided by EC2 [71] to obtain the maximum deflection (δ_{max}) for steel RC members, and it is used in this study to calculate the maximum deflection of FRP RC beams. This equation presumes that elements designed to crack, but may not fully cracked, will perform in a manner between no cracking and full cracking conditions.

$$\delta_{max} = (1 - \zeta)\delta_1^{max} + \zeta\delta_2^{max} \tag{18}$$

where

$$\zeta = 1 - \beta\left(\frac{M_{cr}}{M_a}\right)^m \tag{19}$$

where (β) and (m) are assumed to be equal to 1 and 2, respectively. For uncracked sections, (ζ) equals 0, and (δ_1^{max}) and (δ_2^{max}) are calculated assuming constant uncracked and cracked sectional moments of inertia and are calculated, for four-point bending, as:

$$\delta_1^{max} = \frac{Pa}{24E_c I_g}\left(3L^2 - 4a^2\right) \tag{20}$$

$$\delta_2^{max} = \frac{Pa}{24E_c I_{cr}}\left(3L^2 - 4a^2\right) \tag{21}$$

where (I_g) is the gross moment of inertia and the cracked moment of inertia (I_{cr}) is calculated using elastic analysis principles as:

$$I_{cr} = \frac{bk^3d^3}{3} + nA_f d^2(1 - k)^2 \tag{22}$$

where

$$k = \sqrt{2n\rho_f + (n\rho_f)^2} - n\rho_f \tag{23}$$

in which, (n) is the ratio of the modulus of elasticity of the FRP reinforcement (E_f) to that of the concrete (E_c), (b) and (d) are respectively the effective width and depth of the section, (k) is a factor used to calculate the height of the compressed area of concrete from the top surface. It should be noted that the elastic modulus of concrete is required in the Eq. (20) and (21) and can be calculated using EC2 recommendation as:

$$E_{c,EC2} = 2000\left(\frac{f_c + 8}{10}\right)^{0.3} \tag{24}$$

3.2. 4.2 ACI-440-1R-06 design

3.2.1. Cracking moment

The cracking moment can be calculated using the expression given in Eq. (1), where (f_r) is calculated according to ACI 440.1 R-06 [67] as:

$$f_r = 0.62(f_c)^{1/2} \tag{25}$$

3.2.2. Ultimate capacity

The balanced reinforcement is calculated using the formula given in ACI-440-1R-06 [67] as:

$$\rho_{b,ACI} = 0.85\beta_1\frac{\varepsilon_{cu} f_c}{(\varepsilon_{cu} + \varepsilon_{fu})f_{fu}} \tag{26}$$

where (ε_{cu}) is the ultimate compressive strain of concrete and is assumed to be 0.003 as specified in ACI-440-1R-06, and (β_1) is defined as follows:

$$\beta_1 = 0.85 - 0.05\frac{f_c - 27.6}{6.9} \quad (27)$$

Therefore, if $\rho_f \geq \rho_{b,ACI}$ then the failure is concrete crushing, and the corresponding flexural moment capacity (M_{ult}) is estimated as [67]:

$$M_{ult,ACI} = \rho_f f_f \left(1 - 0.59\frac{\rho_f f_f}{f_c'}\right) bd^2 \quad (28)$$

where f_f, the stress in the FRP rebars, and it is computed as;

$$f_f = \left(\sqrt{\frac{(E_f \varepsilon_{cu})^2}{4} + \frac{0.85\beta_1 f_c}{\rho_f} E_f \varepsilon_{cu}} - 0.5 E_f \varepsilon_{cu}\right) \leq f_{fu} \quad (29)$$

Or else, if $\rho_f \leq \rho_{b,ACI}$ then the beam failure occurs due to the FRP rebar rupture, and flexural moment capacity $(M_{ult,ACI})$ is determined using the following approximate equation:

$$M_{ult,ACI} = A_f f_{fu}\left(d - \frac{\beta_1 c_b}{2}\right) \quad (30)$$

where (c_b) is calculated as;

$$c_b = \left(\frac{\varepsilon_{cu}}{\varepsilon_{cu} + \varepsilon_{fu}}\right) d \quad (31)$$

With regards to the shear capacity, the total shear capacity (V) represents the sum of the shear capacities of the concrete (V_{cf}) and the stirrups (V_f), as stated in the Eq. (14). The concrete contribution in shear (V_{cf}) is calculated using the following equation [67]:

$$V_{cf,ACI} = \frac{2}{5}\sqrt{f_c'} bc \quad (32)$$

where (c) is the depth of the cracked transformed section neural axis. For a singly reinforced rectangular cross section, it is calculated as follows:

$$c = kd \quad (33)$$

where, (k) is calculated from Eq. (23).

The stirrups contribution in shear $(V_{f,ACI})$ is calculated based on the assumption that the limiting strain in the stirrups is 0.4%, therefore the stress in the stirrups is:

$$f_{fv} = 0.004 E_{fv} \quad (34)$$

Similarly, the shear contribution of FRP stirrups can be calculated using Eq. (17). It is worth noting that when steel is used as shear reinforcement in FRP concrete beams, the failure is most probably not a shear failure because the steel stirrups have a very high shear capacity. Thus, shear failure, in this case, is avoided.

3.2.3. Deflection

Typically, the integration of curvatures is used to calculate deflection of RC elements. This process requires a lot of time, making design impractical. In order to easily and precisely estimate the deflection, a simplified design approach using basic elastic analysis models and the effective moment of inertia was developed. This approach, which is based on the use of Branson's equation, has been proved to be successful for steel reinforced members and was subsequently adopted for FRP RC members [23]. In fact, to allow recommendations to be applied to FRP RC members, the ACI 318–08 steel design standard [74] has undergone a number of modifications. Taking references [16–20] as an example, Branson's equation, which aims to overestimate the effective moment of inertia of FRP RC beams, was modified to incorporate a correction factor for predicting the effective moment of inertia and consequently the maximum deflection of FR -RC beams.

The ACI 440.1R-06 [67] code for FRP-RC members recommends the following equation for determining the effective moment of inertia in order to determine the maximum deflection (δ_{max}) at the mid-span for simply supported beams:

$$I_e = \left(\frac{M_{cr}}{M_a}\right)^3 \beta_d I_g + \left[1 - \left(\frac{M_{cr}}{M_a}\right)^3\right] I_{cr} \leq I_g \quad (35)$$

where

$$\beta_d = \frac{1}{5}\left(\frac{\rho_f}{\rho_{b,ACI}}\right) \leq 1 \quad (36)$$

where (M_{cr}) represents the cracking moment calculated from Eq. (1) along with Eq. (25), and (M_a) is maximum moment in beam at stage deflection.

The cracked moment of inertia (I_{cr}) is calculated using Eq. (22). It should be noted that Eq. (35) can be applied, only if $M_a \geq M_{cr}$. As a result, the mid-span deflection for a four-point bending is expressed as follows:

$$\delta_{max} = \frac{Pa}{24 E_c I_e}\left(3L^2 - 4a^2\right) \quad (37)$$

where (a) is the shear span, (P) is the service point load, (L) is the effective span of the beam and (E_c) is the elastic modulus of concrete and is expressed according to ACI 440.1R-06 [67] as:

$$E_{c,ACI} = 4730\sqrt{f_c} \quad (38)$$

4. Results and discussion

In this section, the data collected, according to Table 1, are compared against to the calculation procedures presented by ACI 440.1R-06 [67] and EC2 [71], taking into account the analyses referring to capacity and deflection.

4.1. 5.1 capacity

The test data is compared with calculation procedures presented previously, considering the shear strength with and without stirrups, the flexural behaviour and the cracking moment. It is important to highlight that the comparison is made through the relative error between the calculation model and the experimental one (Prediction/Test-1). In this context, the negative and positive values show that the calculation procedure underestimates and overestimates the capacity, respectively, in comparison with the experimental model.

4.1.1. Shear

Fig. 2 shows the results of the experimental shear capacity of 154 beams without stirrups. The comparison of these results with ACI 440.1R-06 [67] predictions is illustrated in Fig. 2a. In this context, the average value of the relative error, as well as the standard deviation, the variance and regression R^2 were equal to −49.4%, 14.5%, 2.1%, and 0.8124 respectively (Table 2). All predicted results are in favour of safety as the relative errors range between −81.0% and −11.3%, hence, the ACI 440.1R-06 [67] underestimates the capacity of FRP-RC beams without stirrups. Similarly, El Rafai and Abed [38] indicated that ACI 440.1R-06 [67] method was conservative in predicting the shear capacity of BFRP RC beams with mean test-to-predicted ratio value of 1.94 and standard deviation value of 0.43. Interestingly they found that the accuracy of the ACI 440.1R-06 [67] depends on the type of the longitudinal FRP used. For the BFRP, GFRP, and CFRP, the mean test-to-predicted ratio was 1.94, 2.03 and 1.84, respectively, with less scatter prediction for GFRP. Furthermore, Alam and Hussein [42] found similar observation that ACI 440.1R-06 [67] underestimated the shear capacity of CFRP and GFRP RC beams with test-to-predicted value of 1.66. For BFRP RC beams, Issa et al [52] indicated that ACI 440.1R-06 [67] underestimate the capacity and average test-to-predicted value of the

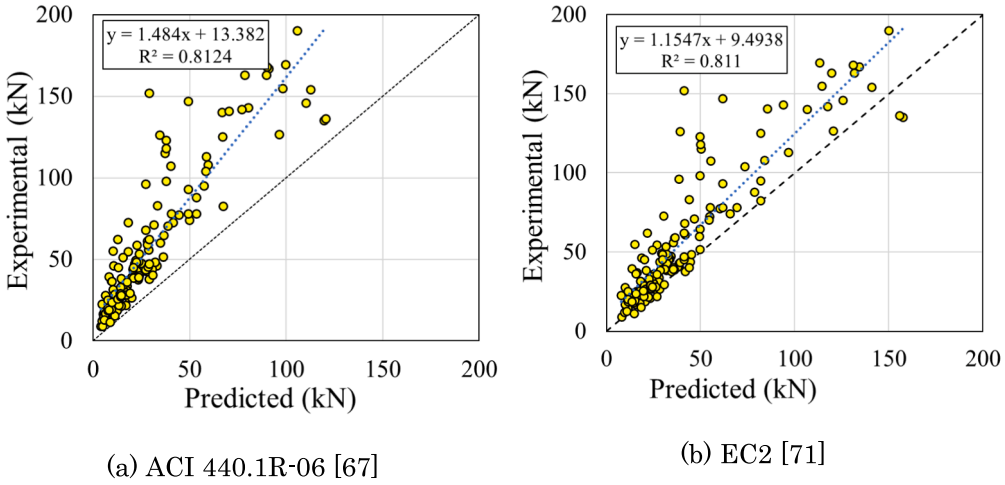

(a) ACI 440.1R-06 [67] (b) EC2 [71]

Fig. 2. Experimental vs. predicted shear strength without stirrups.

investigated beams was 1.45. On the other hand, the comparison with EC2 [71] prediction is shown in Fig. 2b. In this context, the average value of the relative error, standard deviation, variance and regression were equal to −25.1%, 20.1%, 4.0%, and 0.81 respectively. The maximum relative error was equal to 31.2%, while the minimum was equal to −72.8%. EC2 overestimate the shear capacity for only 14 samples (9% of the tested beams). It is important to highlighted that, the Root Mean Squared Error (RMSE) values for ACI 440.1R-06 [67] and EC2 [71] predictions were equal to 35.8 kN and 25.2 kN, respectively. The EC2 [71] provided better match with the test results than those for ACI 440.1R-06 [67] as indicated in the index of agreement value stated in the Table 2.

Fig. 3 presents the comparison between the experimental shear capacity of FRP RC beams with FRP stirrups and the design standards. Considering the shear capacity prediction by ACI 440.1R-06 [67] (Fig. 3a), the average value of the relative error, as well as the standard deviation, variance and regression were equal to −43.1%, 16.1%, 2.6%, 0.74, respectively. The relative errors range between −74.7% and −2.7%. It can be noted that ACI 440.1R-06 [67] underestimates the shear capacity for all test data considered. Similarly, Said et al. [7] stated that ACI 440.1R-06 [67] was overly conservative in predicting the shear capacity of FRP RC beams with FRP stirrups. Issa et al. [52] indicated that ACI 440.1R-06 [67] provided the most conservative shear capacity predictions in comparisons to other international design codes such as

Table 2
Statistical analysis for the predicted and test results.

	Shear- Without Stirrups		Shear-With Stirrups		Flexural Capacity		Cracking Moment		Deflection at 0.67P_u	
	ACI	EC2	ACI	EC2	ACI	EC2	ACI	EC2	ACI	EC2
Correlation Coefficient (R2)	0.81	0.81	0.74	0.71	0.91	0.90	0.59	0.61	0.79	0.78
Pearson's correlation coefficient (R)	0.90	0.90	0.86	0.84	0.96	0.95	0.77	0.78	0.89	0.88
Average Error %	−49.4	−25.1	−43.1	−31.8	−14.8	−8.6	−4.8	8.3	9.4	5.8
Mean Absolut Error MAE	27.69	16.86	76.83	61.65	8.76	6.92	3.34	2.90	4.74	4.15
S.D. %	14.5	20.1	16.1	19.8	15.0	16.5	55.7	64.4	70.5	83.1
Var. %	2.1	4.0	2.6	3.9	2.2	2.7	31.1	41.5	4942	6939
Max Error %	−11.3	31.2	−2.7	16.8	41.2	39.6	226	279	98	703
Min Error %	−81.0	−72.8	−74.7	−69.3	−52.5	−51.8	−77.1	−74.9	−690	−84.1
RMSE	35.80	25.21	95.57	81.14	11.33	9.28	5.36	4.83	6.69	6.24
Index of Agreement	0.76	0.89	0.70	0.79	0.93	0.96	0.86	0.87	0.9	0.93

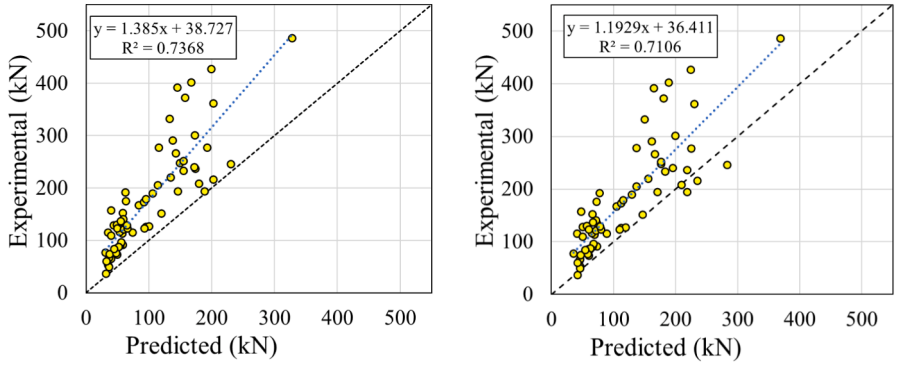

(a) ACI 440.1R-06 [67] (b) EC2 [71]

Fig. 3. Experimental vs. predicted shear strength with stirrups.

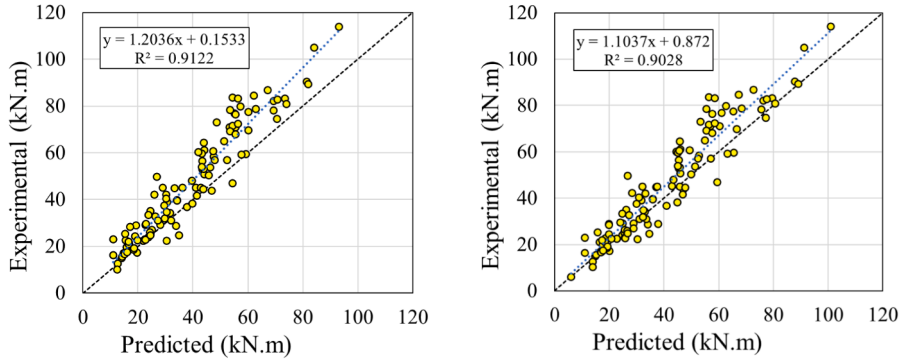

(a) ACI 440.1R-06 [67] (b) EC2 [71]

Fig. 4. Experimental vs. predicted moment capacity.

CSA S806-02 [68]. This is due to the fact that ACI 440.1R-06 [67] is conservative in predicting the shear contribution of concrete and FRP stirrups. Jumaa and Yousif [27] found that ACI 440.1R-06 [67] was very conservative in predicting the shear contribution of BFRP stirrups of the tested beams by 172% on average. With the aid of collected data available in the literature they found that ACI 440.1R-06 [67] was still conservative in predicting the shear contribution of other types FRP stirrups by 69% on average. Hence, they proposed alternative equation to calculate the strain limit value in the stirrups. The comparison of the test results with EC2 [71] is shown in Fig. 3b. The average value of the relative error, standard deviation, variance and regression were equal to −31.8%, 19.8%, 3.9%, and 0.71, respectively. The maximum relative error was equal to 16.8%, while the minimum relative error was −69.3%. The shear capacity of only 4 beams were overestimated by EC2 [71]. Similar to ACI 440.1R-06 [67], EC2 [72] also underestimated the shear capacity of FRP-RC beams with stirrups. The RMSE values for ACI 440.1R-06 [67] and EC2 [71] were equal to 95.6 kN and 81.1 kN, respectively. The EC2 [71] provided better match with the test results than those for ACI 440.1R-06 [67] as indicated in the index of agreement value stated in the Table 2.

4.1.2. Moment

Regarding flexural capacity, 115 experimental results are used and compared with ACI 440.1R-06 [67] and EC2 [71] predictions (Fig. 4). Fig. 4a illustrates comparisons between test results and ACI 440.1R-06 [67] and it can be noted that the average relative error, standard deviation, variance and regression values were equal to −14.8%, 15.0%, 2.2%, and 0.91, respectively, being the relative errors range between −52.5% to 41.2%. In this context, 90% of the predictions were in favour of safety, while 10% of the predictions were against safety. This is in-line with Elgabbas et al. [24] who indicated that ACI 440.1R-06 [67] underestimated the flexural capacity of the six tested beams by 24% on average. On the other hand, considering the EC2 [71] prediction (Fig. 4b), it was verified that the average relative error, standard deviation, variance and regression values were equal to −8.6%, 16.5%, 2.7%, and 0.90, respectively. The relative errors ranged between −51.8% and 39.6%, and EC2 [71] showed an efficacy of 71% of the data collected in favour of safety. Similarly, Shamass and Cashell [1] found that EC2 [71] slightly overestimated the flexural capacity of 40% of the investigated beams and underestimated the capacity of 60% of the studied beams. However, ACI 440.1R-06 [67] was more on the conservative side than the EC2 [71]. As can be seen in the Table 2, the RMSE values for ACI 440.1R-06 [67] and EC2 [71] were equal to 11.3 kN.m and 9.3 kN.m, respectively. The EC2 [71] provided slightly better match with the test results than those for ACI 440.1R-06 [67] as indicated in the index of agreement value stated in the Table 2.

4.1.3. Cracking moment

Fig. 5 illustrates the comparisons between tests and predicted cracking moment, considering a total of 193 test results. Regarding the comparison with the ACI 440.1R-06 [67] (Fig. 5a), the mean relative error value, standard deviation, variance and regression were equal to −4.8%, 55.7%, 31.1%, 0.59, respectively. The relative errors range between −77.1%, and 226.1%. It is important to highlight that 137 (71%) observations were in favor of safety. On the other hand, Elgabbas et al. [24] indicated that ACI 440.1R-06 [67] overestimated the cracking moment by 27% on average. Finally, the comparison with EC2 [71] is shown in Fig. 5b. In this context, the average value of the relative error

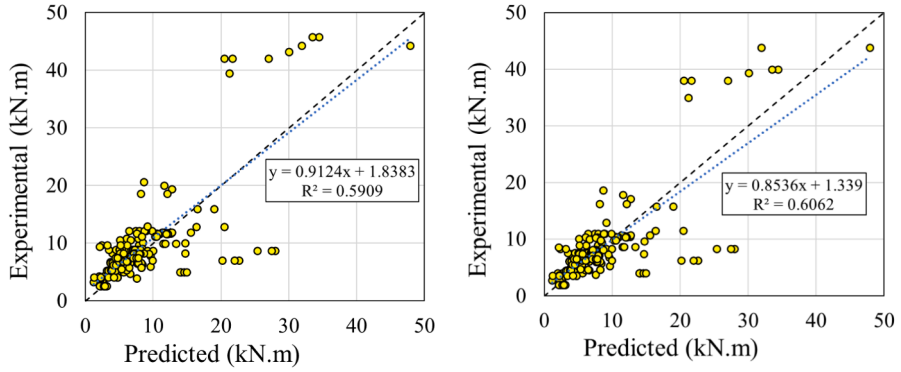

(a) ACI 440.1R-06 [67] (b) EC2 [71]

Fig. 5. Experimental vs. predicted cracking moment.

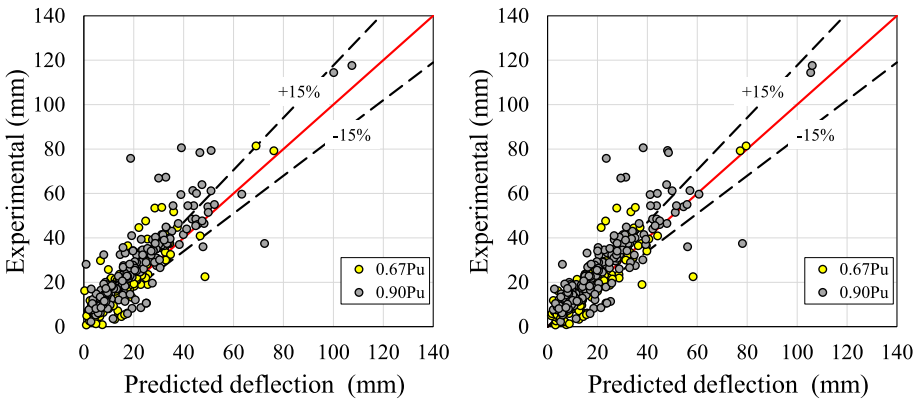

Fig. 6. Experimental vs. predicted deflections.

was equal to 8.23%, while the standard deviation, variance regression obtained the following values 64.4%, 41.5% and 0.61, respectively. The maximum and minimum values of the relative error were equal to 278.7% and −74.9%, respectively. Unlike the ACI 440.1R-06 [67], EC2 [71] was only 60% effective (1 1 5) compared to the tests. This means that the ACI calculation was more effective to predict cracking moment. Shamass and Cashell [1] found that EC2 [71] overestimated the cracking moment of the RC beams reinforced with ribbed surface BFRP by 57% on average and only overestimated the cracking moment by 4.5% on average for sand coated surface BFRP. This indicated the effect of different BFRP surface on the cracking moment predictions.

4.2. Deflection

The deflections obtained from 195 experiments are compared with ACI 440.1R-06 [67] and EC2 [71], considering 67% (assumed service loading), and 90% of the ultimate load (P_u) (Fig. 6). Fig. 6a illustrates comparison between test results and ACI 440.1R-06 [67] predictions, and it can be seen that the average value of the relative error for deflections at $0.67P_u$ was 9.4%. The relative errors ranged between −690% and 98%. Elgabbas et al. (24) found that ACI 440.1R-06 [67] slightly underestimated the deflections at $0.67P_u$. Similarly, Khorasani et al [31] found again that ACI 440.1R-06 [67] underestimated the deflections with average test-to-predicted value 1.24 for beams with high longitudinal reinforcement ratio and 1.38 for beams with low reinforcement ratio. On the other hand, considering the loading at $0.90P_u$, there was an increase in the average relative error at −18.3%. It is important to emphasize that in the total of 195 tests, in comparison with the ACI 440.1R-06 [67], 41 tests presented a relative error of up to −15%, while 21 tests presented a relative error of up to + 15%, considering the loading at $0.67P_u$. As for loading at $0.90P_u$, the number of observations verified were 30 and 11, considering errors of up to −15% and 15%, respectively. The RMSE values for both cases, i.e., $0.67P_u$ and $0.90P_u$, were equal to 6.69 mm and 10.98 mm, respectively.

On the other hand, considering EC2 [71] prediction (Fig. 6b), average values of relative error for deflections at $0.67P_u$ and $0.90P_u$ equal to 5.83% and −13.05%, respectively. The maximum relative errors for the $0.67P_u$ and $0.90P_u$ cases were 703% and 214%, respectively, while the minimum relative errors were −80.5% and −84.1%, considering $0.67P_u$ and $0.90P_u$, respectively. In this context, the number of observations checked for loading at $0.67P_u$, considering the relative errors up to −15% and 15%, were 37 and 34, respectively. These values for the $0.90P_u$ were 36 and 22, for errors up to −15% and 15%, respectively. The calculated values of RMSE were equal to 6.24 mm and 10.48 mm, for deflections at $0.67P_u$ and $0.90P_u$, respectively.

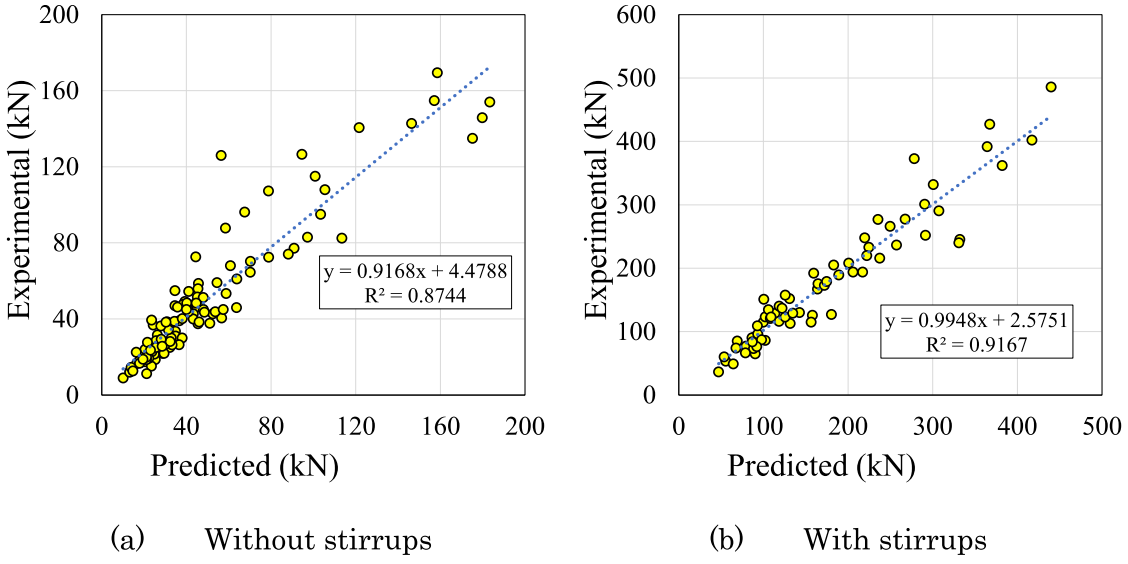

Fig. 7. Regression analysis for shear capacity.

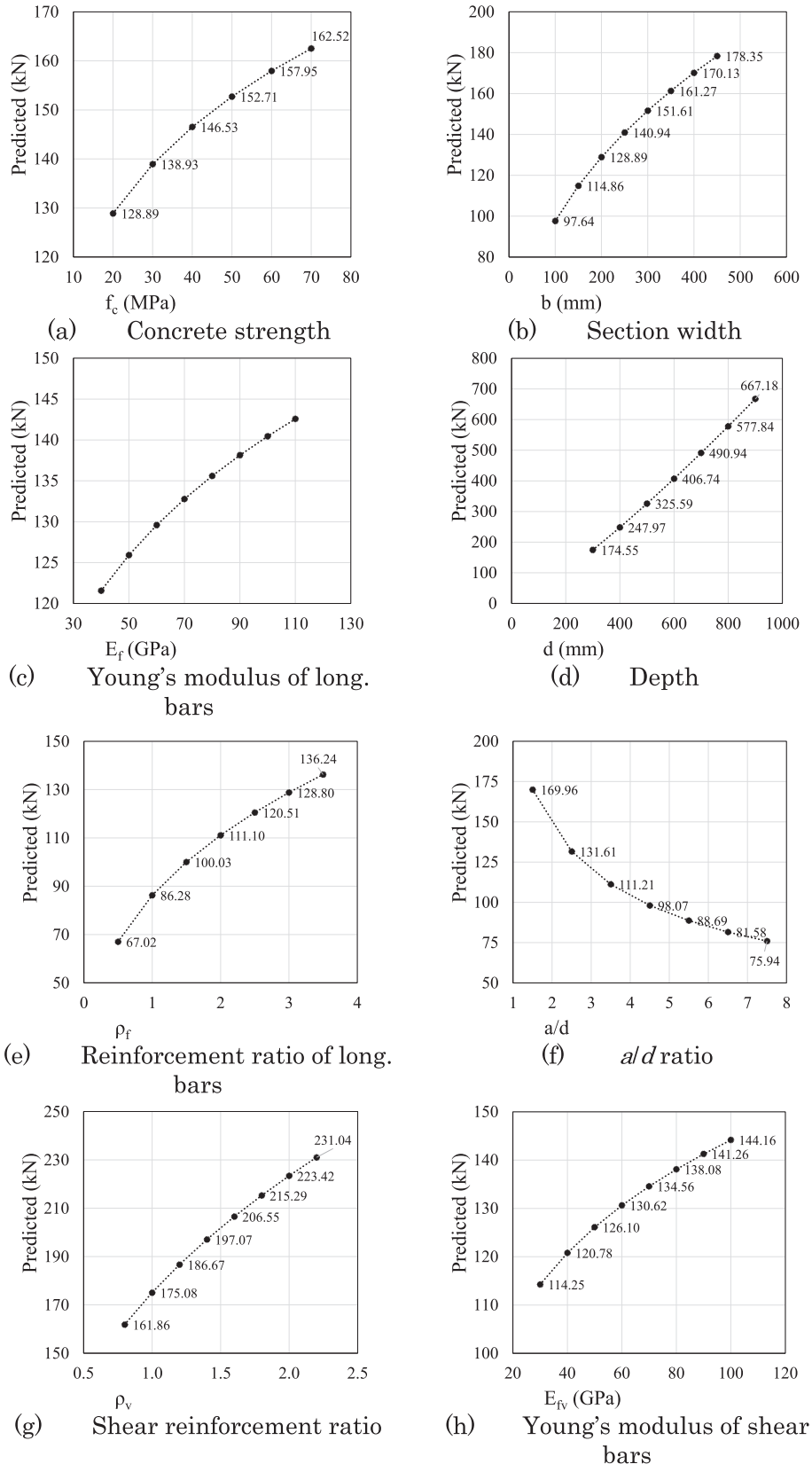

Fig. 8. Influence of parameters for shear capacity with stirrups.

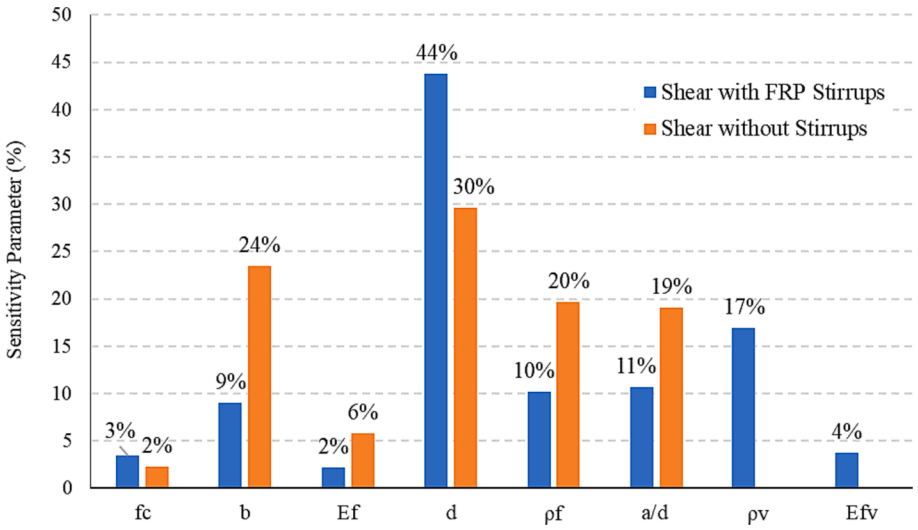

Fig. 9. Sensitivity parameters for the estimated shear capacity of FRP beams.

5. Influence of parameter

A regression analysis is performed to evaluate the influence of geometric and materials parameters on the shear capacity, the flexural capacity and the cracking moment. For this task, the proposed regression equations are analysed by varying one parameter while maintaining the others as constants based on their mean value. For example, to assess the influence of the effective depth on the shear capacity of beams without stirrups, this value was varied from 147 mm to 937.5 mm (the minimum and maximum value from the collected data), while compressive strength of concrete, beam width, elastic modulus of FRP rebars, reinforcement ratio, and a/d ratio were kept constant at mean values of 37.23 MPa, 197.5 mm, 70515.15 mm, 1.016% and 3.23, respectively. The shear capacity was calculated from the regression analysis and the sensitivity analysis parameter of each input parameter is calculated using the Eq. (39) [75,76]:

$$SA_i = \frac{f_{max}(x_i) - f_{min}(x_i)}{\sum_1^n (f_{max}(x_i) - f_{min}(x_i))} \times 100 \tag{39}$$

where $f_{max}(x_i)$ and $f_{min}(x_i)$ are the maximum and minimum estimated output related to the input variable x_i, with all other parameters kept constant at their mean values.

The nonlinear regression analysis was conducted using Multiple Regression with Logarithmic Transformations, a statistical technique used to model the relationship between multiple independent variables and a dependent variable when the relationship is not linear. This approach assumes a power form relationship between the input and output, and the logarithmic transformation is applied to convert the relationship into a linear model with coefficients that need to be determined (representing the indices).

To implement this method, the data transformed using logarithms and then fitted in multiple linear regression model using Excel's Linear Regression data analysis tool to identify the coefficients. Subsequently, the equation was transformed back from its logarithmic form into the original power form.

5.1. Shear capacity

The shear capacity equations with and without stirrups are presented in Eqs. (40)–(41), respectively. The Regression (R^2) is illustrated in Fig. 7. It can be noted that the proposed regression model provided better predictions than the EC2 [71] predictions, particularly for the beam with stirrups for which the regression R^2 is 0.71 and 0.92 for the EC2 [71] prediction and the regression equation, respectively. This is due to the fact that the regression takes into consideration the influence of shear span-to-effective depth ratio (a/d). Therefore, Eq. (40) can be used as design equation alternative to EC2 [71].

$$V = 3.55 \times 10^{-4} \times f_c^{\,0.19} \times b^{0.40} \times E_f^{\,0.16} \times d^{1.22} \times \rho_f^{\,0.36} \times \left(\frac{a}{d}\right)^{-0.50} \times \rho_v^{\,0.35} \times E_{fv}^{\,0.19} \tag{40}$$

$$V = 4.27 \times 10^{-4} \times f_c^{\,0.09} \times b^{0.91} \times E_f^{\,0.26} \times d^{0.78} \times \rho_f^{\,0.41} \times \left(\frac{a}{d}\right)^{-0.66} \tag{41}$$

Fig. 8 illustrates the parameter influence, considering the concrete strength (Fig. 8a), the section width (Fig. 8b), the Young's modulus of longitudinal bars (Fig. 8c), the effective depth (Fig. 8d), the reinforcement ratio of longitudinal bars (Fig. 8e), the a/d ratio (Fig. 8f), the shear reinforcement ratio (Fig. 8g) and the Young's modulus of shear stirrups (Fig. 8h). It can be noted from these graphs that, as expected, the ratio a/d has negative influence on the shear capacity, the larger the ratio and lower the shear capacity, while the other parameters, namely f_c, b, E_f, d, ρ_f, ρ_v and E_{fv}, have positive influence on the shear capacity. Fig. 9 illustrates the importance of each of the parameters on the shear capacity of beams with FRP stirrups. It is possible to state that the parameter with the greatest influence is the effective depth with high sensitivity scores of 44% while shear reinforcement ratio has moderate influence. The parameters of lesser influence are the compressive strength of concrete, Young's modulus of longitudinal and transversal bars with low sensitivity scores of 3%, 2% and 4%, respectively. Hence, the parameters that play an important role in the shear capacity of FRP beams with FRP stirrups are effective depth, shear and longitudinal reinforcement ratio and a/d ratio.

The same analysis was performed regarding the shear capacity of beam without FRP stirrups (Fig. 10). In this context, the investigated parameters are the concrete strength (Fig. 10a), the section width (Fig. 10b), the Young's modulus of longitudinal bars (Fig. 10c), the effective depth (Fig. 10d), the reinforcement ratio of longitudinal bars (Fig. 10e) and the a/d ratio (Fig. 10f). Again, as expected, the ratio a/d has negative influence on the shear capacity, while the other parameters, namely f_c, b, E_f, d, and ρ_f, have positive influence on the shear capacity. As shown in the Fig. 8, the parameter with the greatest influence on shear capacity of FRP RC beams without stirrups is the effective depth with sensitivity score of 30%, while the parameters with the less influence are the concrete strength and Young's modulus of FRP, with sensitivity score of 2% and 6%, respectively. This is expected as the

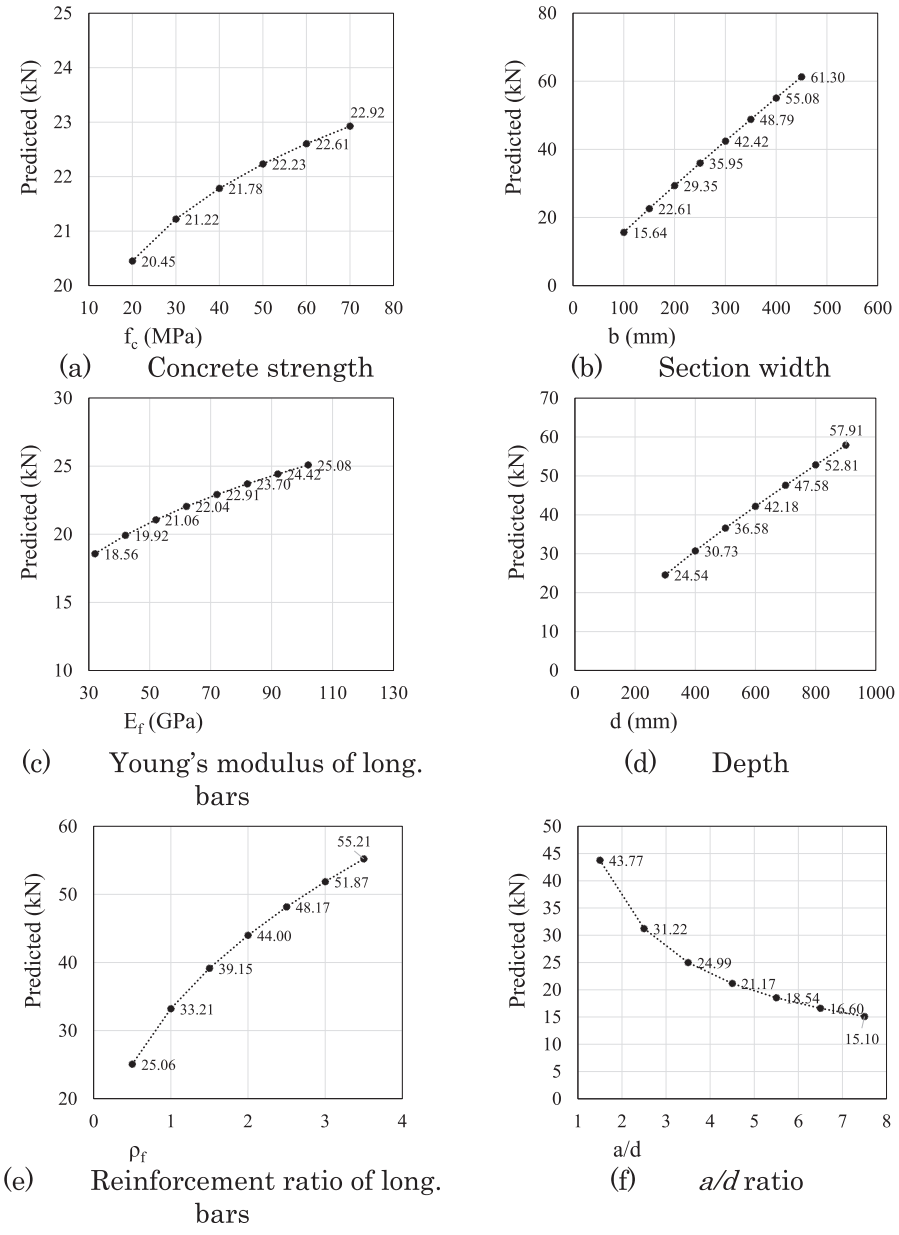

Fig. 10. Influence of parameters for shear capacity without stirrups.

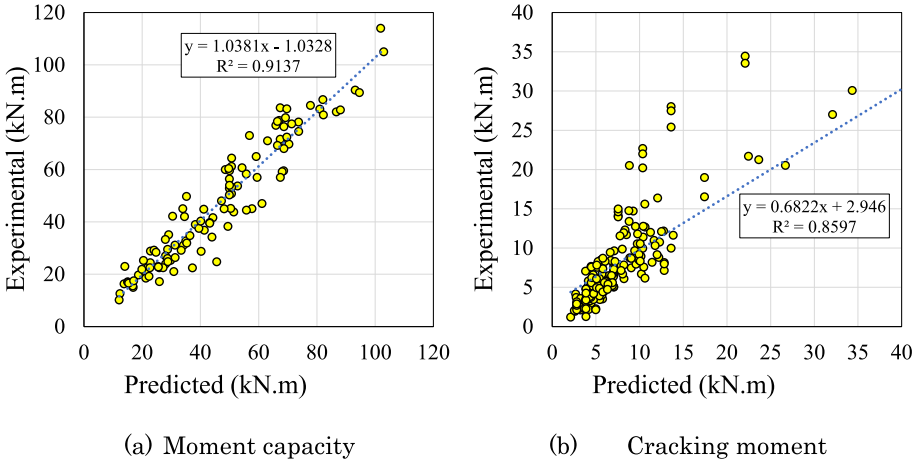

Fig. 11. Regression analysis for moment capacity.

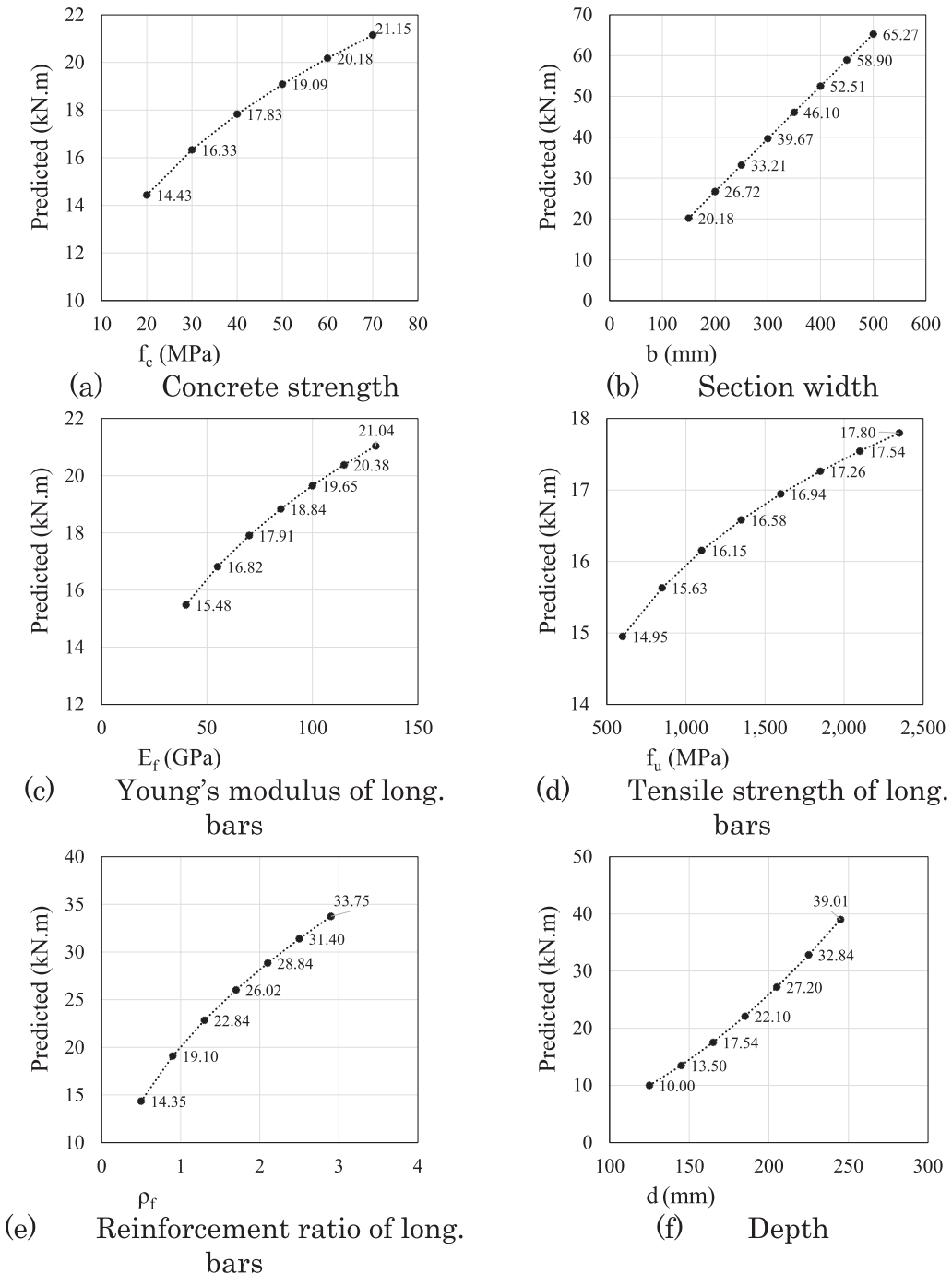

Fig. 12. Influence of parameters for moment capacity.

concrete contribution to shear capacity is minimal due to low elastic modulus of FRP. The reinforcement ratio and a/d ratio have moderate influence on the capacity with sensitivity score of 20% and 19%, respectively. Based on the above discussion it can be concluded that the parameters that play important role in the shear capacity of FRP RC beams are the beam geometry, longitudinal reinforcement ratio and a/d ratio.

5.2. Moment capacity and cracking moment

The regression analysis for the study of parameter influence of flexural capacity and cracking moment is obtained via Eq. (42) and Eq. (43), respectively. The coefficient R^2 is illustrated in Fig. 11. It can be noted that the regression equation for the cracking moment provides better results than EC2 [71] predictions. This is due to the fact that the regression analysis takes into consideration the reinforcement ratio of the rebars while the EC2 [71] cracking moment prediction considers only the beams section geometry and the concrete strength.

$$M = 0.48 \times 10^{-7} \times f_c^{0.30} \times b^{0.97} \times f_u^{0.13} \times E_f^{0.26} \times d^{2.02} \times \rho_f^{0.49} \quad (42)$$

$$M_{cr} = 2.34 \times 10^{-6} \times b^{0.18} \times h^{2.29} \times f_c^{0.34} \times \rho_f^{0.31} \quad (43)$$

The parameter influence analysis considering the moment capacity (Fig. 12) is performed considering the concrete strength (Fig. 12a), section width (Fig. 12b), the Young's modulus of longitudinal bars (Fig. 12c), the tensile strength of longitudinal bars (Fig. 12d), the

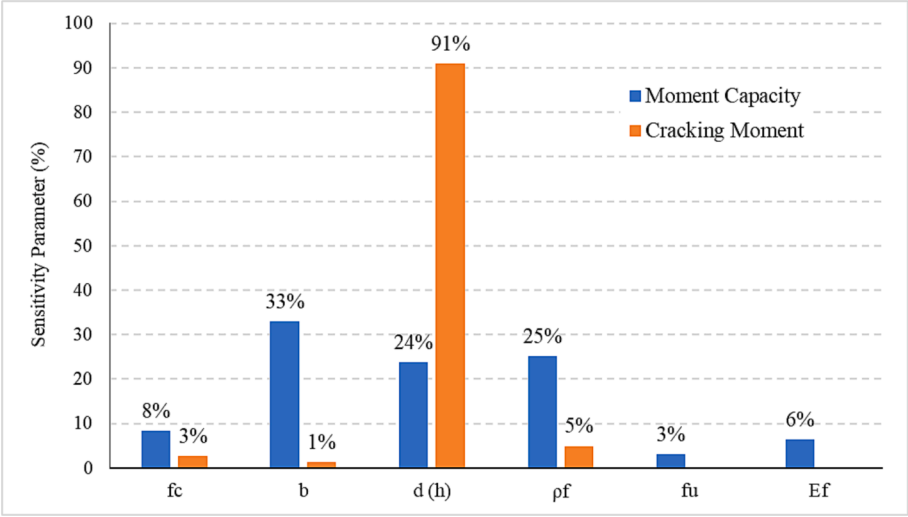

Fig. 13. Sensitivity parameters for the estimated moment capacity and cracking moment of FRP beams.

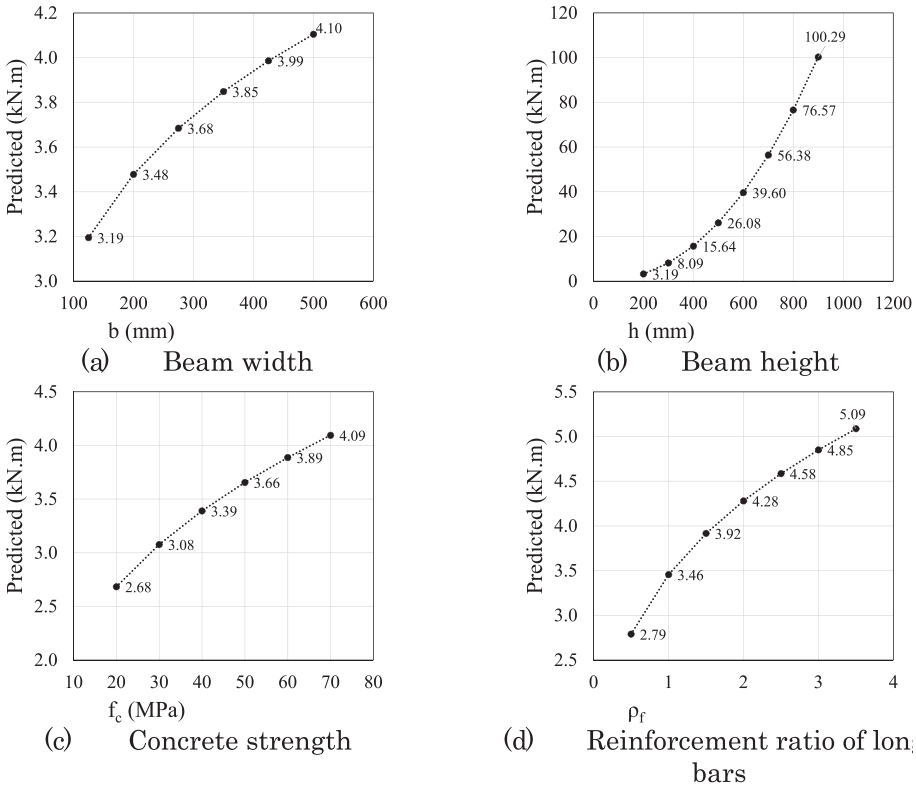

Fig. 14. Influence of parameters for cracking moment.

reinforcement ratio of longitudinal bars (Fig. 12e) and the effective depth (Fig. 12f). It can be seen that all considered parameters have positive influence on the moment capacity, however, each parameter has different impact on the moment capacity based on their sensitivity score shown in Fig. 13. According to Fig. 13, the parameters with the most influenced on the moment capacity were the beam effective depth, width, and reinforcement ratio, with sensitivity score of 24%, 33% and 25%, respectively, while the parameter that least influenced on the moment capacity was the tensile strength of longitudinal bars, with sensitively score of only 3%. This is expected for beam with concrete crushing failure as the moment capacity is governed by the crushing strain of concrete not by the tensile strength of the FRP rebars.

Fig. 14 illustrates the variation of the parameters as a function of the cracking moment. This analysis was carried out considering the beam width (Fig. 14a), the beam height (Fig. 14b), the concrete strength (Fig. 14c) and the reinforcement ratio of longitudinal bars (Fig. 14d). Similarly, all these parameters have a positive influence on the cracking moment, however, the height of the beam is the most pronounced influence with 91% of sensitivity score (Fig. 13) and the width is the least influence on the cracking moment.

Table 3
Summary of the reliability analysis calculated according to EN 1990 [77].

Failure	n	$\overline{b}$	$k_{d,n}$	k_n	V_r	γ_{M0}
Flexural	115	1.121	3.04	1.64	0.271	1.45
Shear-without stirrups	154	1.292	3.04	1.64	0.372	1.63
Shear-with stirrups	67	1.420	3.04	1.64	0.371	1.65

6. Reliability analysis based on Annex D EN 1990

In this section, reliability analysis based on Annex D EN 1990 (2002) [77] has been conducted to assess the reliability of the EC2 [71] formulations and propose a partial safety factor for the flexural and shear capacity of RC members reinforced with FRP. The statistical evaluation of the EC2 [71] prediction model is done herein based on the collected test data.

Table 3 illustrates the key statistical parameters, including the number of data, n, the design fractile factor (ultimate limit state), $k_{d,n}$, the Characteristic fractile factor, k_n the average ratio of test to resistance model predictions based on the least squares fit to the data, $\overline{b}$, the combined coefficient of variation incorporating both resistance model and basic variable uncertainties, V_r, and the partial safety factor for resistance γ_{M0}. The COV of geometric dimensions of the concrete beam is 0.04 for the width and the height [78], while it is 0.015 for the diameter of the longitudinal FRP rebars and stirrups [79]. The COV of the tensile strength of FRP, elastic modulus of FRP and concrete compressive strength were assumed equal to 0.05 [70], 0.05 [70] and 0.18 [80], respectively. Performing First Order Reliability Method (FORM) in accordance with the Eurocode target reliability requirements, the partial factors γ_{M0} were evaluated. As can be seen from Table 3, the partial factor for the FRP reinforced beams failed in flexural and shear without and with FRP stirrups are 1.45, 1.63 and 1.65, respectively.

7. Conclusions, recommendations, and prospects

In this paper, a total of 336 test data from 53 references on ultimate load and 195 experimental data points on load–deflection in 36 references was collected for supported FRP RC beams with high and normal concrete strength, and with and without transverse reinforcement. This experimental database was used and compared with the ACI 440.1R-06 and EC2 prediction. To date, there is no European design code for the FRP RC members and hence this paper presented, for the first time, a comprehensive design proposal for the FRP RC members according to EC2 framework both in shear and flexural. Regression analysis was conducted to discuss the influence of parameters on the shear and moment capacities, as well as the cracking moment. The main findings throughout this study were:

- Both FRP design guides ACI and EC2 underestimate the shear capacity of FRP RC beams. The parameters that most influenced the shear capacity with stirrups were the effective depth and shear reinforcement ratio, that is, the greater of these parameters, the greater the shear capacity. On the other hand, for beams without stirrups, the parameters with the greatest influence were the beam width, effective depth, reinforcement ratio and a/d ratio. The parameters with the lowest influence on the shear capacity FRP RC beams with and without stirrups were the Young's modulus of longitudinal bars and the concrete strength.
- The flexural capacity of FRP RC beams showed that both ACI and EC2 provided conservative moment capacity predictions, however, greater number of ACI predictions were in favor of safety. Regarding the analysis of the parameter influence on the moment capacity, the most important parameters were the effective depth, width and reinforcement ratio, while for the cracking moment the greatest influence was the height of the beam.
- Regarding the deflection, both design codes presented 74 (38%) and 121 (62%) observations that overestimated and underestimated the calculation of the deflection of FRP RC beams, respectively.
- Regarding the EC2 predictions, the R^2 and RMSE values were 0.81 and 25.2 kN, respectively for shear capacity without stirrups, while they were 0.71 and 81.1 kN for shear capacity with stirrups. For flexural capacity prediction, the R^2 and RMSE were 0.90 and 9.3 kN.m, respectively. For deflection predictions at service loading, the R^2 and RMSE were 0.78 and 6.24 mm, respectively.
- The reliability analysis was conducted, and it was suggested to use the partial safety factor of 1.45, and 1.65 for flexural and shear capacities according to EC2, respectively.
- The main limitation of this study is that short-term deflections were studied. However, the long-term deflections should be also investigated, and the FRP RC design code predictions should be verified, which can be a future study.
- The serviceability requirements investigated in this study were limited by the deflections' predictions. The crack width of the FRP RC members has not been investigated and compared with the design code in this study which can be suggested as future study.

CRediT authorship contribution statement

Rabee Shamass: Methodology, Conceptualization, Investigation, Supervision, Writing – original draft. **Ikram Abarkan:** Methodology, Investigation, Conceptualization, Writing – original draft. **Felipe Piana Vendramell Ferreira:** Methodology, Validation, Investigation, Writing – original draft.

Declaration of Competing Interest

The authors declare that they have no known competing financial interests or personal relationships that could have appeared to influence the work reported in this paper.

Data availability

Data will be made available on request.

References

[1] Shamass R, Cashell KA. Experimental investigation into the flexural behaviour of basalt FRP reinforced concrete members. Eng Struct 2020 Oct;1(220):110950.
[2] Apostolopoulos CA, Papadakis VG. Consequences of steel corrosion on the ductility properties of reinforcement bar. Constr Build Mater 2008 Dec 1;22(12):2316–24.
[3] Ožbolt J, Balabanić G, Kušter M. 3D Numerical modelling of steel corrosion in concrete structures. Corros Sci 2011 Dec 1;53(12):4166–77.
[4] Broomfield J. Corrosion of steel in concrete: understanding, investigation and repair. Crc Press; 2003 Jul 9..
[5] Adam MA, Said M, Mahmoud AA, Shanour AS. Analytical and experimental flexural behavior of concrete beams reinforced with glass fiber reinforced polymers bars. Constr Build Mater 2015 Jun;1(84):354–66.
[6] Theriault M, Benmokrane B. Effects of FRP reinforcement ratio and concrete strength on flexural behavior of concrete beams. J Compos Constr 1998 Feb;2(1):7–16.
[7] Said M, Adam MA, Mahmoud AA, Shanour AS. Experimental and analytical shear evaluation of concrete beams reinforced with glass fiber reinforced polymers bars. Constr Build Mater 2016 Jan;15(102):574–91.
[8] Reinforcing Concrete Structures with Fibre Reinforced Polymers. Design Manual No. 3. Intelligent Sensing for Innovative Structures Canada; 2007.
[9] Abed F, Al-Mimar M, Ahmed S. Performance of BFRP RC beams using high strength concrete. Composites Part C: Open Access 2021 Mar;1(4):100107.
[10] Bashtannik PI, Kabak AI, Yakovchuk Y. The effect of adhesion interaction on the mechanical properties of thermoplastic basalt plastics. Mech Compos Mater 2003 Jan;39(1):85–8.
[11] Duo Y, Liu X, Liu Y, Tafsirojjaman T, Sabbrojjaman M. Environmental impact on the durability of FRP reinforcing bars. J Build Eng 2021 Nov;1(43):102909.
[12] Lu C, Yang Y, He L. Mechanical and durability properties of GFRP bars exposed to aggressive solution environments. Sci Eng Compos Mater 2021 Jan 1;28(1):11–23.
[13] Mohamed OA, Al Hawat W, Keshawarz M. Durability and mechanical properties of concrete reinforced with basalt fiber-reinforced polymer (BFRP) bars: towards sustainable infrastructure. Polymers 2021 Apr 26;13(9):1402.

[14] Lee LS, Jain R. The role of FRP composites in a sustainable world. Clean Techn Environ Policy 2009 Sep;11(3):247–9.
[15] Barris C, Torres L, Turon A, Baena M, Catalan A. An experimental study of the flexural behaviour of GFRP RC beams and comparison with prediction models. Compos Struct 2009 Dec 1;91(3):286–95.
[16] Benmokrane B, Masmoudi R. Flexural response of concrete beams reinforced with FRP reinforcing bars. Struct J 1996 Jan 1;93(1):46–55.
[17] Brown VL, Bartholomew CL. Long-term deflections of GFRP-reinforced concrete beams. InFirst International Conference on Composites in InfrastructureNational Science FoundationNational Sicence Foundation 1996 Jan.
[18] Masmoudi R, Theriault M, Benmokrane B. Flexural behavior of concrete beams reinforced with deformed fiber reinforced plastic reinforcing rods. Struct J 1998 Nov 1;95(6):665–76.
[19] Pecce M, Manfredi G, Cosenza E. Experimental response and code models of GFRP RC beams in bending. J Compos Constr 2000 Nov 1;4(4):182–90.
[20] Toutanji H, Deng Y. Deflection and crack-width prediction of concrete beams reinforced with glass FRP rods. Constr Build Mater 2003 Feb 1;17(1):69–74.
[21] Balendran RV, Tang WE, Leung HY, Nadeem A. Flexural behaviour of sand coated glass-fiber reinforced polymer (GFRP) bars in concrete. In29th Conference on "Our World in Concrete & Structures 2004 Aug.
[22] Tomlinson D, Fam A. Performance of concrete beams reinforced with basalt FRP for flexure and shear. J Compos Constr 2015 Apr 1;19(2):04014036.
[23] Al-Sunna R, Pilakoutas K, Hajirasouliha I, Guadagnini M. Deflection behaviour of FRP reinforced concrete beams and slabs: An experimental investigation. Compos B Eng 2012 Jul 1;43(5):2125–34.
[24] Elgabbas F, Vincent P, Ahmed EA, Benmokrane B. Experimental testing of basalt-fiber-reinforced polymer bars in concrete beams. Compos B Eng 2016 Apr;15(91):205–18.
[25] Zhang L, Sun Y, Xiong W. Experimental study on the flexural deflections of concrete beam reinforced with Basalt FRP bars. Mater Struct 2015 Oct;48(10):3279–93.
[26] Kassem C, Farghaly AS, Benmokrane B. Evaluation of flexural behavior and serviceability performance of concrete beams reinforced with FRP bars. J Compos Constr 2011 Oct 1;15(5):682–95.
[27] Jumaa GB, Yousif AR. Size effect on the shear failure of high-strength concrete beams reinforced with basalt FRP bars and stirrups. Constr Build Mater 2019 Jun;10(209):77–94.
[28] Pawłowski D, Szumigała M. Flexural behaviour of full-scale basalt FRP RC beams–experimental and numerical studies. Procedia Eng 2015 Jan;1(108):518–25.
[29] Rafi MM, Nadjai A, Ali F, Talamona D. Aspects of behaviour of CFRP reinforced concrete beams in bending. Constr Build Mater 2008 Mar 1;22(3):277–85.
[30] Razaqpur AG, Isgor BO, Greenaway S, Selley A. Concrete contribution to the shear resistance of fiber reinforced polymer reinforced concrete members. J Compos Constr 2004 Oct;8(5):452–60.
[31] Khorasani AM, Esfahani MR, Sabzi J. The effect of transverse and flexural reinforcement on deflection and cracking of GFRP bar reinforced concrete beams. Compos B Eng 2019 Mar;15(161):530–46.
[32] Ashour AF. Flexural and shear capacities of concrete beams reinforced with GFRP bars. Constr Build Mater 2006 Dec 1;20(10):1005–15.
[33] Alsayed SH, Al-Salloum YA, Almusallam TH. Performance of glass fiber reinforced plastic bars as a reinforcing material for concrete structures. Compos B Eng 2000 Oct 1;31(6–7):555–67.
[34] Wang L, Zhang J, Huang C, Fu F. Comparative study of steel-FRP, FRP and steel-reinforced coral concrete beams in their flexural performance. Materials 2020 Jan;13(9):2097.
[35] Sun ZY, Yang Y, Qin WH, Ren ST, Wu G. Experimental study on flexural behavior of concrete beams reinforced by steel-fiber reinforced polymer composite bars. J Reinf Plast Compos 2012 Dec;31(24):1737–45.
[36] Barris C, Torres L, Comas J, Mias C. Cracking and deflections in GFRP RC beams: an experimental study. Compos B Eng 2013 Dec;1(55):580–90.
[37] Oh H, Moon DY, Zi G. Flexural characteristics of concrete beams reinforced with a new type of GFRP bar. Polym Polym Compos 2009 May;17(4):253–64.
[38] El Refai A, Abed F. Concrete contribution to shear strength of beams reinforced with basalt fiber-reinforced bars. J Compos Constr 2016 Aug 1;20(4):04015082.
[39] Kim CH, Jang HS. Concrete shear strength of normal and lightweight concrete beams reinforced with FRP bars. J Compos Constr 2014 Apr 1;18(2):04013038.
[40] Kalpana VG, Subramanian K. Behavior of concrete beams reinforced with GFRP BARS. J Reinf Plast Compos 2011 Dec;30(23):1915–22.
[41] Erfan AM, Algash YA, El-Sayed TA. Experimental & analytical flexural behavior of concrete beams reinforced with basalt fiber reinforced polymers bars. Int J Sci Eng Res 2019;10(8):297–315.
[42] Alam MS, Hussein A. Experimental investigation on the effect of longitudinal reinforcement on shear strength of fibre reinforced polymer reinforced concrete beams. Can J Civ Eng 2011 Mar;38(3):243–51.
[43] Massam L. The behaviour of GFRP-reinforced concrete beams in shear (Doctoral dissertation).
[44] Yang JM, Min KH, Shin HO, Yoon YS. Behavior of high-strength concrete beams reinforced with different types of flexural reinforcement and fiber. InAdvances in FRP Composites in Civil Engineering 2011 (pp. 275-278). Springer, Berlin, Heidelberg.
[45] Matta F, Nanni A, Hernandez TM, Benmokrane B. Scaling of strength of FRP reinforced concrete beams without shear reinforcement. InFourth International Conference on FRP Composites in Civil Engineering (CICE2008) Zurich, Switzerland 2008 Jul 22 (pp. 1-6).
[46] Zhao W, Maruyama K, Suzuki H. Shear behavior of concrete beams reinforced by FRP rods as longitudinal and shear reinforcement. InRilem Proceedings 1995 Aug 23 (pp. 352-352). Chapman & Hall.
[47] Thiagarajan G. Experimental and analytical behavior of carbon fiber-based rods as flexural reinforcement. J Compos Constr 2003 Feb;7(1):64–72.
[48] Duranovic N, Pilakoutas K, Waldron P. Tests on concrete beams reinforced with glass fibre reinforced plastic bars. Non-metallic (FRP) reinforcement for concrete structure. 1997 Oct 14;2:479-86.
[49] Tariq M, Newhook JP. Shear testing of FRP reinforced concrete without transverse reinforcement. InProceedings, Annual Conference of the Canadian Society for Civil Engineering 2003 Jun (pp. 1330-1339).
[50] Yost JR, Gross SP, Dinehart DW. Shear strength of normal strength concrete beams reinforced with deformed GFRP bars. J Compos Constr 2001 Nov;5(4):268–75.
[51] Tureyen AK, Frosch RJ. Shear tests of FRP-reinforced concrete beams without stirrups. Struct J 2002 Jul 1;99(4):427–34.
[52] Issa MA, Ovitigala T, Ibrahim M. Shear behavior of basalt fiber reinforced concrete beams with and without basalt FRP stirrups. J Compos Constr 2016;20(4):04015083.
[53] Ali I, Thamrin R, Abdul AA, Noridah M. Diagonal shear cracks and size effect in concrete beams reinforced with glass fiber reinforced polymer (GFRP) bars. Appl Mech Mater 2014;621:113–9.
[54] Zeidan M, Barakat MA, Mahmoud Z, Khalifa A. Evaluation of concrete shear strength for FRP reinforced beams. InStructures Congress 2011;2011:1816–26.
[55] Nagasaka T, Fukuyama H, Tanigaki M. Shear performance of concrete beams reinforced with FRP stirrups. Special publication 1993 Sep;1(138):789–812.
[56] Maruyama K, Zhao WJ. Flexural and shear behaviour of concrete beams reinforced with FRP rods. Corrosion and corrosion protection of steel in concrete. 1994 Jul: 1330-9.
[57] Vijay PV, Kumar SV, GangaRao HV. Shear and ductility behavior of concrete beams reinforced with GFRP rebars. InPROCEEDINGS OF THE 2ND INTERNATIONAL CONFERENCE ON ADVANCED COMPOSITE MATERIALS IN BRIDGES AND STRUCTURES, ACMBS-II, MONTREAL 1996 1996.
[58] Maruyama K. Size Effect in Shear Behavior of FRP Reinforced Concrete Beams advanced Composite Materials in Bridges and Structures. CSCE 1996:227–34.
[59] Alkhrdaji T, Wideman M, Belarbi A, Nanni A. Shear strength of GFRP RC beams and slabs. InProceedings of the international conference, composites in construction-CCC 2001 Oct 10 (pp. 409-414).
[60] Niewels J. Zum Tragverhalten von Betonbauteilen mit Faserverbundkunststoff-Bewehrung (Doctoral dissertation, Aachen, Techn. Hochsch., Diss., 2008).
[61] Tottori S, Wakui H. Shear capacity of RC and PC beams using FRP reinforcement. Special Publication 1993 Sep;1(138):615–32.
[62] Nakamura H, Higai T. Evaluation of shear strength of concrete beams reinforced with FRP. Doboku Gakkai Ronbunshu 1995 Feb 20;1995(508):89–100.
[63] Mizukawa Y, Sato Y, Ueda T, Kakuta Y. A study on shear fatigue behavior of concrete beams with FRP rods. Non-metallic (FRP) reinforcement for concrete structure. 1997;2:309-16.
[64] Lubell A, Sherwood T, Bentz E, Collins M. Safe shear design of large wide beams. Concr Int 2004 Jan 1;26(1):66–78.
[65] El-Sayed AK, El-Salakawy EF, Benmokrane B. Shear strength of concrete beams reinforced with FRP bars: design method. ACI Special Publication 2005 Nov;6:230.
[66] El-Sayed AK, El-Salakawy EF, Benmokrane B. Shear strength of FRP-reinforced concrete beams without transverse reinforcement. ACI Mater J 2006 Mar 1;103(2):235.
[67] Guide for the design and construction of concrete reinforced with FRP bars. Farmington Hills, MI: American Concrete Institute; 2006.
[68] Design and Construction of Building Structures with Fibre-Reinforced Polymers. Canadian Standards Association Mississauga, Ont; 2012.
[69] Konstrukcii betonnye, armirovannye polimernoj kompozitnoj armaturoj. Pravila proektirovaniya. Obshchiye Tekhnicheskiye Usloviya [Concrete structures reinforced with fibre-reinforced polymer bars. Design rules], Standartinform [Publisher], Moscow; 2017 (in Russian).
[70] FRP reinforcement in RC structures. Lausanne: International Federation for Structural Concrete; 2007.
[71] Eurocode 2: Design of concrete structures, European Committee for Standardization; 2004.
[72] Fico R, Prota A, Manfredi G. Assessment of Eurocode-like design equations for the shear capacity of FRP RC members. Compos B Eng 2008 Jul 1;39(5):792–806.
[73] Feeser WK, Brown VL. Guide examples for design of concrete reinforced with FRP bars. Special Publication 2005 Oct;1(230):935–54.
[74] ACI Committee. Building code requirements for structural concrete (ACI 318-08) and commentary. American Concrete Institute.
[75] Huynh AT, Nguyen QD, Xuan QL, Magee B, Chung T, Tran KT, et al. A machine learning-assisted numerical predictor for compressive strength of geopolymer concrete based on experimental data and sensitivity analysis. Appl Sci 2020;10(21):7726.
[76] Lavercombe A, Huang X, Kaewunruen S. Machine learning application to eco-friendly concrete design for decarbonisation. Sustainability 2021;13(24):13663.
[77] European committee for standardization, EN 1990: Eurocode – Basis of structural design, (n.d.).
[78] Feng L, Li PD, Huang XX, Wu YF. Reliability-Based Design Analysis for FRP Reinforced Compression Yield Beams. Polymers 2022;14(22):4846.
[79] Aghamohammadi R, Nasrollahzadeh K, Mofidi A, Gosling P. Reliability-based assessment of bond strength models for near-surface mounted FRP bars and strips to concrete. Compos Struct 2021;272:114132.

[80] Qiu W, McCann F, Espinos A, Romero ML, Gardner L. Numerical analysis and design of slender concrete-filled elliptical hollow section columns and beam-columns. Eng Struct 2017;131:90–100.
[81] Narváez NS, Rojas NR, Evangelista Jr F. Reliability analyses of shear strengthened RC beams with externally bonded fiber reinforced polymer. Mater Struct 2020;53 (2):31.
[82] Taki A, Firouzi A, Mohammadzadeh S. Life cycle reliability assessment of reinforced concrete beams shear-strengthened with carbon fiber reinforced polymer strips in accordance with fib bulletin 14. Struct Concr 2018;19(6): 2017–28.
[83] Firouzi A, Taki A, Mohammadzadeh S. Time-dependent reliability analysis of RC beams shear and flexural strengthened with CFRP subjected to harsh environmental deteriorations. Eng Struct 2019;196:109326.
[84] Borzovič V, Gajdošová K, Halvonik J, Gregušová N. Partial factor for the shear resistance model in the 2nd generation of Eurocode 2 for GFRP reinforced concrete members. Eng Struct 2023;285:116005.